Wearable inertial sensors for centre of mass stability changes during the incremental shuttle walk test

by

Abdullah Alshehri

Supervisor

Dr. David Hobbs

Thesis
Submitted to Flinders University
for the degree of

Master of Engineering Science (Biomedical)

College of Science & Engineering

5/7/2022

TABLE OF CONTENTS

ABSTRACT

Wearable inertial sensors are cheap and portable devices that have recently changed the measurement of the postural sway and balance; Several studies have investigated the inter-sensor and test-retest reliability or the validity of the balance in healthy individuals or those at risk. Current studies have shown inertial sensors to be reliable in static standing eyes open and able to distinguish the old from the young or fallers from non-fallers in terms of their amplitude of Medio-lateral sway, gait velocity turn speed, of Measuring during walking, stepping, or sit-to-stand have been used either in natural or other environments remains questionable. The accuracy of the discrimination between the age or fall risk remains undetermined, especially focusing on the ability of the sensors to be able to differentiate between the postural sway components in natural settings compared to the clinical state with the goal towards prevention of falls or near falls. In this type of data collection with sensors, the practical application by previous researchers has shown some of the limitations in the measurement of postural sway during movement, the reliability, and validity, thus making this unclear. Most of the studies also identified how postural stability is usually maintained in regards to the situation where the center of mass ('COM') is located over the base of support ('BOS') while dynamic (moving) or alternatively while static (in a stable position). The methodology entails collecting accelerometer data using the Inertial Measurement Unit appropriately placed on the pelvis. Necessary computation of the accelerometer output and displacement done. Required assumptions were highlighted, and data pre-processing was then described regarding the main results and limitations. The amplitude differences (cm) were recorded for each of the subjects in the first and second trials. Both positive and negative were observed in the trials. The positive corresponds to the increasing amplitude that occurs during increasing walking speed. Likewise, the negative values show decreased amplitude related to decreasing walking speed. That average sway was noted to provide a similar trend in both increasing and decreasing forms. The difference in regards to the sign was noted to be constant. However, an exception was recorded in the last subject. There was an explanation in null of the difference in the amplitude. The apparent limitation concerning the study was in terms of having non-idealist for the accelerometers, changes in the hypothesis supporting the horizontality of the y-axis during walking, and the presence of the soft-tissue artifact introduced by sliding movement to cause time-varying orientation leading to errors during the double integration are all important limitations noted to influence the outcome of the study.

DECLARATION

I certify that this thesis:

1. does not incorporate without acknowledgment any material previously submitted for a degree or diploma in any university
2. and the research within will not be submitted for any other future degree or diploma without the permission of Flinders University; and
3. to the best of my knowledge and belief, does not contain any material previously published or written by another person except where due reference is made in the text.

Signature of student.....A. Alshehri.....

Print name of student.....Abdullah Alshehri…

Date.....5/7/2022.....

I certify that I have read this thesis. In my opinion it is fully adequate, in scope and in quality, as a thesis for the degree of Master of Engineering Science (Biomedical). Furthermore, I confirm that I have provided feedback on this thesis and the student has implemented it partially.

Signature of Principal Supervisor .....

Print name of Principal Supervisor ... David Hobbs.....

Date ...6th June 2022.....

ACKNOWLEDGEMENTS

First and foremost, I am extremely grateful to my supervisors Dr. David Hobbs and PhD student Nicky Baker for their invaluable advice, continuous support, and patience during my Master study. Their immense knowledge and plentiful experience have encouraged me in all the time of my thesis.

LIST OF FIGURES

1. INTRODUCTION

1.1 Background

Human balance in the standing position has been assessed quantitatively via posturographic examination. This type of examination is a systematic measurement & interpretation of quantities which have been considered to be characteristics exhibited by postural sway when humans are in an upright position (Caruso et al. 2021). This evaluation has been done both in natural and clinical settings to assess the fall risks, especially in geriatric subjects, to evaluate those balance-related disabilities objectively. Furthermore, the Posturography study is not only helpful in geriatric individuals but for those in sports to assess the subtle differences concerning the balance performances of athletes (Hubble et al. 2015). Over the years, Posturography has evolved with the contribution of increasing interest in the study of balance, making it easier for the researcher to understand various dimensions related to balance. Methods that are now being used to study the variables have also evolved (Mobbs et al. 2022). For instance, what was traditionally used to evaluate the body's postural sway was the 'force-plate' focusing on the trajectory of the center of Pressure. However, this has changed because of the weight during transportation and the cost of conducting the study, which is impractical in clinical settings and sports centers. The inexpensive and lightweight features of the miniaturized Inertial Measurement Units or Magneto Inertial Measurements Units (MIMUs) make their device of choice that is now recommended or used in posturography (Murray & Shankar 2017). Those devices can easily be worn by the subjects on any part of the body depending on which type of study is being used, i.e., with the use of elastic belts or bands. More than one could be on the body; however, the number of sensors to be worn or the part of the body they are placed in depends on the application considered. What each sensor contains or elements also depends on their purpose or functions (Pang et al. 2019). For instance, wearable inertial sensors are equipped with accelerometers, gyroscopes, and magnetometers. Some are designed for 3D measurement, which includes motion and gravity.

Euler angles, such as "roll," "pitch," and "yaw," are often used to describe rotations around three orthogonal axes in the sensor-fixed three-dimensional frame of the turn. Local magnetic field amplitude and direction could be measured using a magnetometer, which uses a three-axes frame to represent components of the magnetic field (Rantalainen et al. 2020). This standard three-axes frame is used to measure the accelerometer, gyroscope and magnetometer sensors on the sensing IMU. Since the validity of IMU-based balance evaluations for the gold standard force platform is unknown, wearable sensors have not yet established a standard in posturography.

As long as they are proved correct, wearable sensors for balancing measures would be excellent since they are low-cost and readily movable in multiple contexts. However, fall risk

assessment by wearable sensors is a contentious issue in the balance control literature. Some wearable devices have been used to sense the fall risk assessment in older individuals or provide insights into detecting the near fall, such as the slips, trips, stumbles, or temporary loss of balance. Some come in the form of trackers for the geriatric individuals for helping to track or monitor various physical changes or activities indicators, which will then be analysed for detecting the fall detection or prediction (Hubble et al. 2015). This is peculiar for use in patients with certain pathologies or disabilities that have been found to affect the human balance performance. Those disorders include Parkinson's disease (PD) or Multiple Sclerosis.

In addition to the ongoing need for rehabilitation specialists to have accurate balance outcome measurements, there is an increasing interest in creating wearable devices especially for the market of "active ageing." For both healthy and ill persons. Balance training using wearable sensors and bio feedback is a promising research subject in this context. The benefits of wearable sensor-based balance and gait training on balance, gait and functional performance have been studied in a number of randomized controlled trials involving both healthy and sick populations. In addition, a study looked into smartphone apps that performed body balancing tests. This study builds on past work by evaluating many studies that use wearable sensors to detect postural balance and provides a complete overview of the most widely reported uses.

Balance postural control is necessary for staying upright, moving efficiently, and responding to environmental obstacles. Balance enhances one's quality of life and well-being. On the other hand, balance problems might lead to a near-fall or a fall, resulting in bodily, psychological, or social effects and death in some situations. By "taking corrective measures to recover stability," a person avoids falling after losing their footing due to a trip or stumble (Su et al. 2020). Even though near falls are a strong predictor of falls, little study has been done on them, hence the path from near falls to actual falls remains unclear. The healthcare system does not pay attention to people in the community who have near-falls but do not sustain an injury. In spite of this, they are the group most in need of fall prevention measures. Until recently, falling was the strongest predictor of falling again.

Recent research has revealed clinical tests that can distinguish near-fallers from fallers and non-fallers, including single-leg stance, lunge, and tandem walk five steps (Caruso et al. 2021; Murray & Shankar 2017; Pang et al. 2019; Rantalainen et al. 2020). While there is evidence that falls history is linked to changes in test performance, little is known about the role of postural sway in these outcomes. The body's movement over the base of support, known as postural sway, is a sign of balance. Wearable inertial sensors have surpassed traditional ways of measuring the speed, direction, and amplitude of postural sway using force plates or motion capture in gait laboratories, with the new

interest in monitoring standing balance and gait. In comparison to laboratory equipment, inertial sensors are less expensive, more portable, and allow postural sway measurements to be obtained in any situation appropriate for the population under study. Wearable inertial sensors are also compact, light, and unobtrusive and can be attached to the body with tape, belts, or straps (Ghislieri, et al. 2019). Sensor data can be recorded on three axes, enabling extensive three-dimensional information on tiny changes in postural sway in both static and dynamic settings. Sway measurements taken using inertial sensors can distinguish between different age groups and healthy individuals, and adults with Parkinson's disease, multiple sclerosis, and other neurological diseases. Using a wearable inertial sensor to determine the risk of falling is more sensitive than clinical testing using the timed up and go method (Luinge & Veltink 2004). However, the accuracy and reliability of inertial sensors for measuring postural sway remain unknown, especially in otherwise healthy people who experience near-falls and falls.

Fall risk assessments are majorly focused on patients with chronic or neurological diseases or the elderly with less regard or consideration for the young adults, which studies have now identified to be living with many disorders considered geriatric conditions (McAndrew et al. 2012). Advancements in technology have changed the mode of assessments whereby wearable devices have taken the order of the day, especially for detecting variables common in patients with a high risk of falling or near fall (Haagsma et al. 2020). Posturography has influenced the field with the evolution of detection mode using wearable devices in natural and laboratory-induced settings. There are different types of devices; however, understanding how to use them properly with the highest forms of accuracy remains a major challenge. In addition, there are current unclear findings from different studies conducted with different subjects or populations (Hussen & Jleta 2015). For example, those studies that have been undertaken on the high-risk population while they are at home or in a controlled setting have not yet proven to give a specified accurate approach to measure an excellent postural sway when the human state is in an upright, balanced position.

Currently, the understanding of the measurement of the postural sway with the sensors is still related to the ability of those sensors to be able to detect those different movement and motion conditions found to be associated with the moving body parts and their measurement axes, which is known to be aligned with the direction of motion (Mobbs et al. 2022). Sensors with accelerometers with other sensors that can estimate the short linear displacement of the body parts remain the suitable devices for the fall risk assessment, which remain the main goal of the study; however, there is still common error found to be around 4.5% regardless of the health status of the individual (Neville et al. 2015). This gives a questionable interpretation of the quantities that characterized the postural sway, usually targeted and measured during an upright stance. Getting this done during an incremental

shuttle walk test remain in an upright position remain a challenge that needs to be explored, especially in fall risk geriatric or young adult patient. Studying such scenarios with the wearable sensors during normal gait or movement with the incremental shuttle walk test has never been done. This remains a challenge or research gap that needs to be explored, especially when the device Is placed on the pelvis at the L3, L4, or L5. Before fall risk or near fall risk and how it needs to be prevented can be properly understood, it is important for the researchers or experts to understand the factors that influence human stability during working or when exposed to the various perturbations.

1.2 Problem Statement

Chronic or neurological diseases and old age tend to increase fall risk among individuals. Fall risk detection wearable sensors have thus been developed to assess the balance needs of these categories of patients. IMU is a common medical assessment tool used in such assessments. The devices are in different designs, which are wearable on any part of the subject's body parts. Nevertheless, recent years witnessed an increase in geriatric conditions among younger patients. The implication is an increase in the number of patients whose fall risks should be accurately predicted. Consequently, it is imperative to determine whether IMUs can accurately be used to differentiate between fallers and non-fallers. In this regard, the existing wearable sensors' performance needs to be investigated, and the test protocols are developed to ensure that they are reliable when used among all categories of patients with balance challenges. The current study fills this gap.

1.3 Objectives

The study's main objective was to;

Investigate the accuracy of wearable inertial sensors for centre of mass stability, in predicting patient's ability to balance postural control

The specific objectives include;

i. To investigate the performance of common wearable sensors and develop test protocols adaptable in assessing their performance.
ii. To identify the variables, parameters and outcomes associated with wearable sensors and evaluate them for enhanced performance.
iii. To test whether the protocol developed can be adapted in actual data collection from individuals with postural sway and balance challenges.

2. LITERATURE REVIEW

Body sway measurements have proven to be a vital reference point for risk assessment of falls in humans. Inexpensive wearable inertial sensors have become a valuable tool for this assessment (Baker et al. 2021; Mobbs et al. 2022). The measure has been used to discriminate between different age groups and among adults that are healthy or living with Parkinson's disease or other disorders of a neurological nature (Baker et al. 2021). Understanding how good balance can lead to improved quality of life and how deficient balance can lead to falls or near falls is critical for health providers. The latter can often result in adverse physical, mental, or social outcomes, including death, especially among the elderly or those with neurological disorders (Haagsma et al. 2020).

The inertial sensor, accelerometers, or other inertial measurement units ('IMUs') are generally considered wearable sensors that are portable, flexible, and inexpensive alternatives to those camera-based motion analysis systems (Hubble et al. 2015). Moreover, those sensors have proven valuable compared to those clinically-diagnosed analyses or measurements. Those sensors have proven to be of better choice because they require little space for normal operation without significant post-processing procedures to get the required outcome (Hubble et al. 2015).

Earlier studies have collectively highlighted the need for the use of wearable sensors to evaluate those changes associated with the patient's balance and respective gait pattern or offer an important mode of screening individuals for different risk factors that could be linked with Parkinson's disease or fall (Hubble et al. 2015; Rantalainen et al. 2020; Su et al. 2020). However, some research focused only on healthy individuals or robots to understand the human motion, near fall or fall, and position estimation using sensors (Neville et al. 2015; Alvarez et al. 2018). In contrast, others target both populations to understand how near falls or falls occur in standard settings to provide needed information that will help plan intervention or preventive programs to prevent the rate of falls in everyday settings (Ghislieri et al. 2019). Nevertheless, there is still a need for more scientifically-rigorous future research before making more concrete recommendations for utilizing the specified devices as the needed predictive instruments for clinical populations (Hubble et al. 2015).

Despite the practical use of the sensors in measuring the postural sway during movement, the reliability and validity remain somewhat unclear (Neville et al. 2015; Baker et al. 2021). Postural stability is noticed to be maintained in the situation where the center of mass ('COM') is located over the base of support ('BOS') while dynamic (moving) or alternatively while static (in a stable position) (Baker et al. 2021). The margin of stability ('MOS') is the dynamic stability amount during gait, and this is assessed by utilizing the velocity and position of the COM over the BOS (Baker et al. 2021). While there has been the investigation of the MOS during the time of normal gait, so far, there has

been limited investigation during increased walking speeds, such as, namely, during the incremental shuttle walk test ('ISWT') (Szczegielniak et al. 2018). The incremental shuttle walk test has been considered a symptom-limited but externally paced test conducted on a 10m course. There is a gradual or incremental increase in the individual's walking speed every minute (Evans & Goldstein, 2014). This gradual increase in the speed is done until fatigued sets in. Fatigue plays an essential role in influencing individual postural stability; hence utilizing wearable sensors to monitor those changes as the speed increases and fatigue develops thus provides researchers with a better understanding of the possible association with increased risk of falls, especially among the elderly (Evans & Goldstein 2014; Baker, et al. 2021). However, those features studied by the wearable sensors during normal gait or movements have not been studied during the incremental shuttle walk test (Evans & Goldstein, 2014). This is a research gap that requires exploration. What this is in mind, the current review chapter explores the literature on changes to postural stability by assessing the impact of fatigue on the COM and MOS. At the same time, subjects use wearable inertial sensors on L4.

Understanding maintenance of human stability while working and being exposed to perturbations remain critical in preventing falls. Studies that have tried to explore such aspects of postural stability mainly focused on investigating the role of MOS or the COM. A systematic review by Baker et al. (2021) has shown the usefulness of inertial sensors in various movements such as walking and stepping or while sitting to stand to help discriminate fallers from non-fallers. However, as highlighted above, the accuracy of the discrimination remains unclear, according to Baker et al. (2021). In one of the reviewed studies, Doheny et al. (2012) were shown to focus on using a single body-worn accelerometer as the wearable device considered to be low cost and portable for balance assessment which is also critical while assessing the fall risks, while others such as Alvarez et al. (2018) used accelerometers to explore different aspects of postural stability by monitoring the moving body parts with the measurement axes and its alignment with the direction of motion—achieving an excellent postural sway, which is considered to be the movement of the COM when a human's main upright balance remains an important factor in human stability across the different clinical populations, especially those with neurological issues such as Parkinson's disease, aged adults with a higher risk of fall and those with head injuries (Neville et al. 2015).

Posturography remains the systematic measurement and interpretation of quantities that characterize postural sway in an upright stance (Ghislieri et al. 2019). Since the incremental shuttle walk test is to be done in an upright position, measuring or estimating the fall risk of geriatric patients or reviewing the evaluation of the balance-related conditions, including Parkinson's and stroke, using the wearable sensors for reading the subtle differences related to the balance or stability. Inertial sensors can now be used for recording the individual postural sway by measuring the trajectory of the center of pressure ('COP') (Ghislieri et al. 2019). We understand that postural instability or gait

disability remains a major threat to the independence and well-being of the elderly or those with Parkinson's disease because of the association with an increased risk of falls or fall-related injuries (Hubble et al. 2015). However, the lack of sensitivity for accurate and consistent clinical assessments of those situations has reinforced the interest in using different wearable sensors as portable and inexpensive alternatives for researchers and clinicians.

In terms of the reliability of the balance, Baker et al. (2021) noticed a moderate to good reliability in cases of dynamic balance. At the same time, validity for the static and dynamic balance was also reviewed, and it was noticed that this was moderate for both types of balance. The synthesis of the studies revealed that the wearable sensor checked out for the amplitude of mediolateral sway, the gait velocity, step length, or the turning speed (Baker et al. 2021). Apart from this, the wearable inertial sensor's measurement of the postural sway in healthy patients provides the needed real-time data in the natural environment. Studies synthesised by the authors show differences in the component of the postural sway compared to those recorded from the altered performance in clinical tests. Such help creates a notable target for preventive interventions for cases of falls or the near falls. From the studies reviewed by Baker et al. (2021), it was noted that most of the studies used different sensors, while some used accelerometers for the measurements. Those sensors were noted to vary in terms of the type, number, positions, fixation, or calibration methods (Baker et al. 2021). The inertial sensors used in those studies have inbuilt gyroscopes, which help measure the rotational velocity data. The part of the body where those used sensors are placed depends on the purpose. Still, for this study, most of the positions and fixation were those that are placed on the lumbar spine since that is the region that is closest to the centre of gravity of the body, which is critical in measure of the body balance, and this was noted to produce greater accuracy compared to the thoracic sensors. To further reinforce the understanding of the role of the MOS during human walking, changes during stable and unstable conditions need to be explored.

McAndrew et al. (2012) focused on quantifying the pseudorandom anterior-posterior and mediolateral oscillations impact the dynamic walking stability. This was computed for the margins of stability for each of the trials. It was noted that those subjects might have been engaged in controlling their foot placement and stability during those perturbation conditions (McAndrew et al. 2012). Using the foot placement to control the magnitude of the margin of stability during walking was based on the definition of stability (McAndrew et al. 2012). However, maintaining the minimum MOS in a more mediolateral way could significantly influence controlling the stability during walking simply because it was noted that there is always an increase in MOS variability in perturbations situations (McAndrew et al. 2012). This means that using the wearable sensors during perturbations for recording the MOS variability has a role in uncovering instability issues, especially in adults. Based on the goal of the study, one of the kinds of literature reviewed further proven the importance

of wearable inertial sensors in the measurement of the COM of postural sway by examining its validity and sensitivity with respect to other methods utilising the health group population (Neville et al. 2015).

The moving body part has its measurement axes aligned with the direction of motion (Alvarez et al. 2018). Therefore, sensors can detect those different movement and motion conditions. Based on the experiments conducted by Alvarez et al. (2018) utilising the accelerometers, which are also important wearable sensors, it was found that it's possible to use that type of sensor to estimate the short linear displacements of the body parts being measured. With this type of approach or measurements, a typical error of around 4.5% was observed, especially during general conditions. As a study reviewed considered both the dynamic and static stability during walking (McAndrew et al. 2012), especially during the motion kinematic condition, which has been considered a key factor in the estimation of the performance since the dynamic response of the accelerometer can thus influence the final outcome. Accelerometers and sensors with gyroscopes inbuilt are now being used in real-time measurement of the body motion Spatio-temporal parameters, especially with the key consideration to the low consumption and cost or the associated easy connectivity (Alvarez et al. 2018).

Hubble et al. (2015) evaluated different articles that measured the standing balance and the walking stability using different types of wearable sensors among those already diagnosed with Parkinson's disease. One significant apparent finding from the review was that there is still a need for more high-quality studies to be conducted to comprehend the benefit of the wearable sensors for identifying the PD-related symptoms and fall risk assessment in a different population (Hubble 2015). Despite the associated merits of those wearable sensors used in the reviewed studies, it was noted among 81% of the studies that there were apparent differences in the measurement, especially in regards to the assessments of standing balance or walking stability among those different groups of PD persons or among the healthy control groups. Understandably, falls among the elderly have created severe health concerns, resulting in hip fractures, fatalities, or traumatic brain injuries (Pang et al. 2019). On the other hand, activities of daily life ('ADL') of those groups of people monitored have provided the information needed to categorise them to be of high risk of falling. This monitoring has been done with the continuous and obstructive use of wearable sensors (Pang et al. 2019). The findings also emphasised how that information has helped identify those issues that could serve as the target for the fall prevention programs or interventions. Apart from this, Pang et al. (2019) was able to systematically review various other studies, which further revealed that wearable devices were able to be used to detect artificially induced new falls with very high accuracy, sensitivity, and specificity in the range of 85.7%-100% within the controlled settings, however, in the case of the daily life and laboratory testing, such findings could be different (Pang et al. 2019). From the

reviewed studies, wearable sensors or devices were used to measure data needed to distinguish near falls from ADLs, especially in young adults (Pang et al. 2019).

Some of those studies used an approach similar to the incremental walking method since the patient or individual is made to either walk gradually, stand, rise from sitting, or descend from the standing position, which could create a fall situation (Pang et al. 2019). Some studies conducted studies that use sensors to distinguish near falls from the actual falls or near falls from those considered to be of high-risk populations, especially those with the Parkinson's disease who are already diagnosed for a certain period (the idea was to use 6 different hazard conditions) where about 29 missteps were provoked to train the decision tree (Pang et al. 2019).

Risk assessments are majorly focused on those with chronic or neurological diseases or the elderly, but in some situations, young adults have been put for assessment where the systematic review by Pang et al. (2019) has shown that wearable devices can also be used for the detection of the laboratory-induced near falls in them in a controlled setting and with high accuracy. However, there are unclear findings regarding the accuracy of wearable sensors in detecting the near falls among the older adults or those considered to be among the high-risk population while they are at home or in other major community settings (Pang et al. 2019).

3. METHODOLOGY

This section describes the processing followed in computing the sway starting from the accelerometer data collected by one Inertial Measurement Unit placed on the pelvis. This section is organized as follows: first of all, a description of the accelerometer output and how the displacement is computed starting from these measurements is given; after that, the main assumptions are discussed; then, the data-pre-processing is described, and the main results are listed and analysed; finally, the limitations are discussed.

3.1 Understanding the Sensor

3.1.1 Test protocol:

The sensor (METAMTIONR r0.4) was already selected by colleagues in the College of Nursing and Health Sciences and data was also provided. The goal to understand data and analysis it so to reach this point we should knowing how sensor work by doing specific test using record video for test protocol and then comparing data output for each test to sea differences.

3.1.1.1 Normal walk:

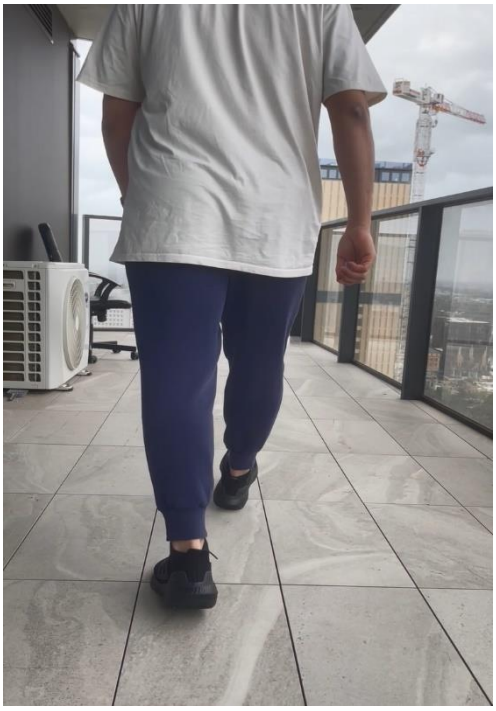

Figure 1. Normal walk test

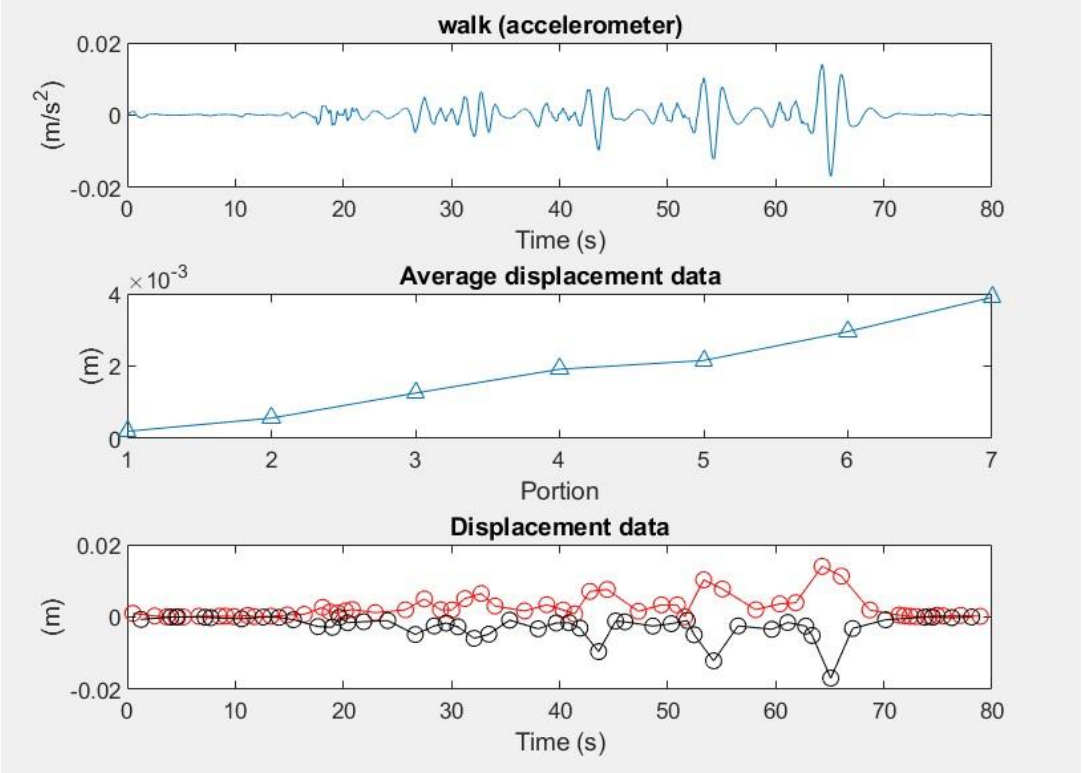

Figure 2: Normal walk data

Figure 2 is a graphical representation of a normal walk test as recorded by the sensor. It focuses on acceleration, which is presented in meters per second. It also records average displacement data, and the displacement data. In terms of acceleration, the Y axis goes right and left, which is consistent with a normal walk. An increase the meters covered per second translate into increased right and left movements sway recorded by the IMU. For instance, while 10m/s, the right and left movements are not as intense as when the pace increases to 30m/s. Further intensity is recorded at 70 m/s. A consistent increase in acceleration translates in increased average displacement data. Similarly, there is an increase in the displacement data. For instance, a comparison between the accelerometer and displacement data reveal that the right and left movements in the former are equally reflected in the latter. In this regard, there is stability in movement.

3.1.1.2 Slight sideway:

Figure 3: Slight sideway test

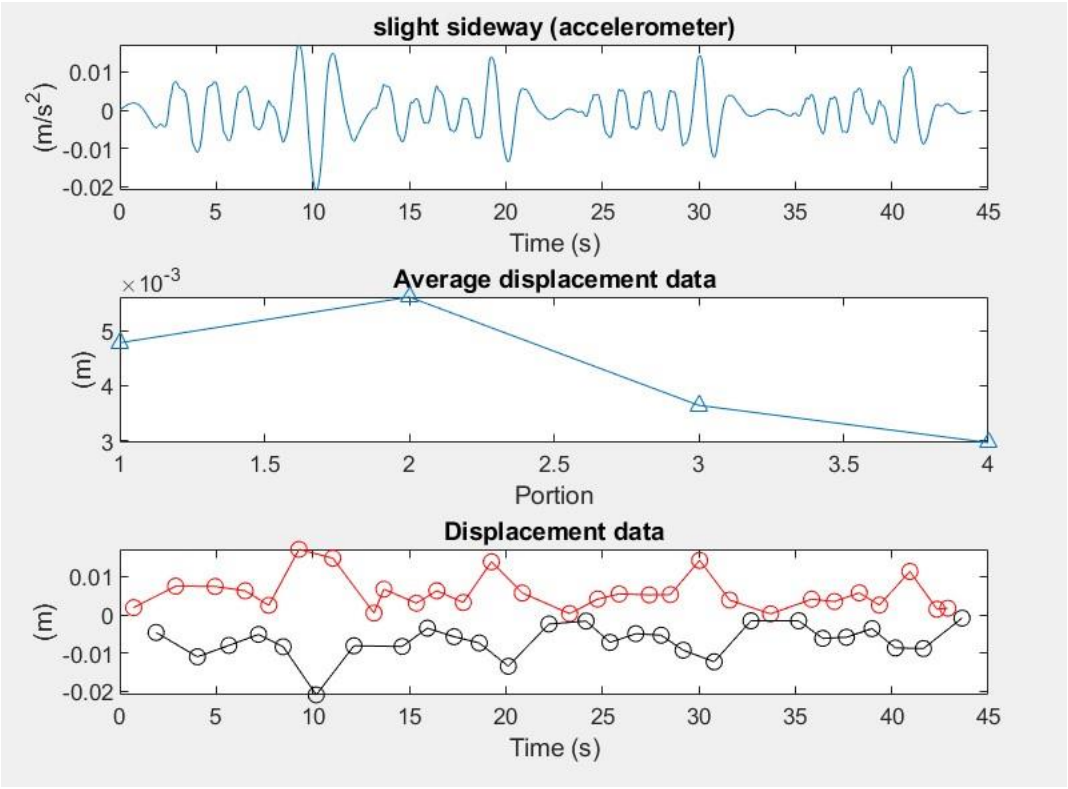

Figure 4: Slight sideway data

Figure 4 summarizes data recorded by the IMU with regard to the sideway movements of its wearer. It focuses on the wearer's slight sideways movement, the average displacement data obtained from the movement, and the displacement data. In terms of slight sideway acceleration, it is evident that the first movement is intense. As a result, the Y axis right and left movements are wider compared to

subsequent movements. In this regard the m/s covered at 10s, which is the onset of the sideways movement, extends more right and left from the Y axis compared to when the IMU wearer is moving at 20m/s, 30m/s, and 40m/s. Movements in these subsequent accelerations consistently decreases. The average displacement data in Figure 4 demonstrates the downward trajectory of the right and left movements as acceleration increases. A similar trend is evident in the displacement data provided, which equally indicate a downward trend in the movements from the Y axis.

3.1.1.3 Hop (L):

Figure 5: Hop (L) test

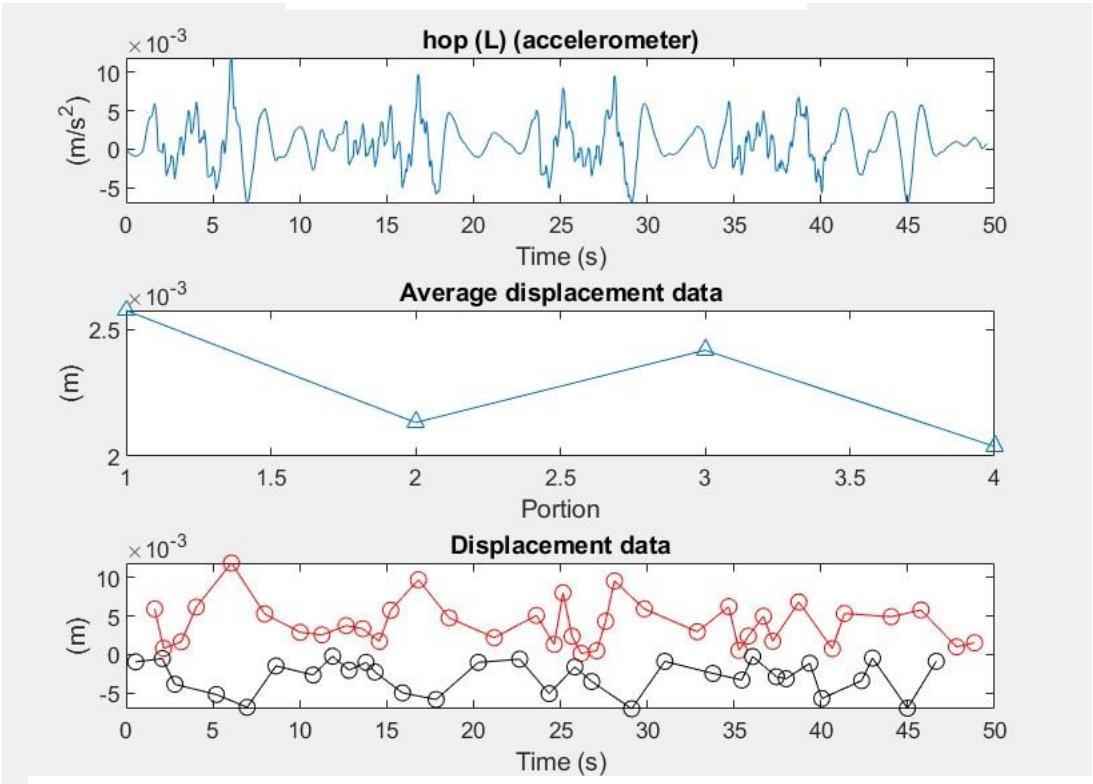

Figure 6: Hop (L) data

Figure 6 summarises the activity in Figure 6, which entails a left hop test. It focuses on the IMU's wearer's hop (L) acceleration, the average displacement data, and displacement data. Unlike in normal walk test and slight sideway test, acceleration (m/s) predictably results in an increase in right and left movements from the Y axis. An increased hop (L) acceleration however decreases right and left movements on the Y axis. The subsequent increases in acceleration result in additional intervals of increase and decrease in the right and left movements on the Y axis. The displacement data equally summarizes these movements as maximum and minimum.

3.1.1.4 Hop (R):

Figure 7: Hop (R) test

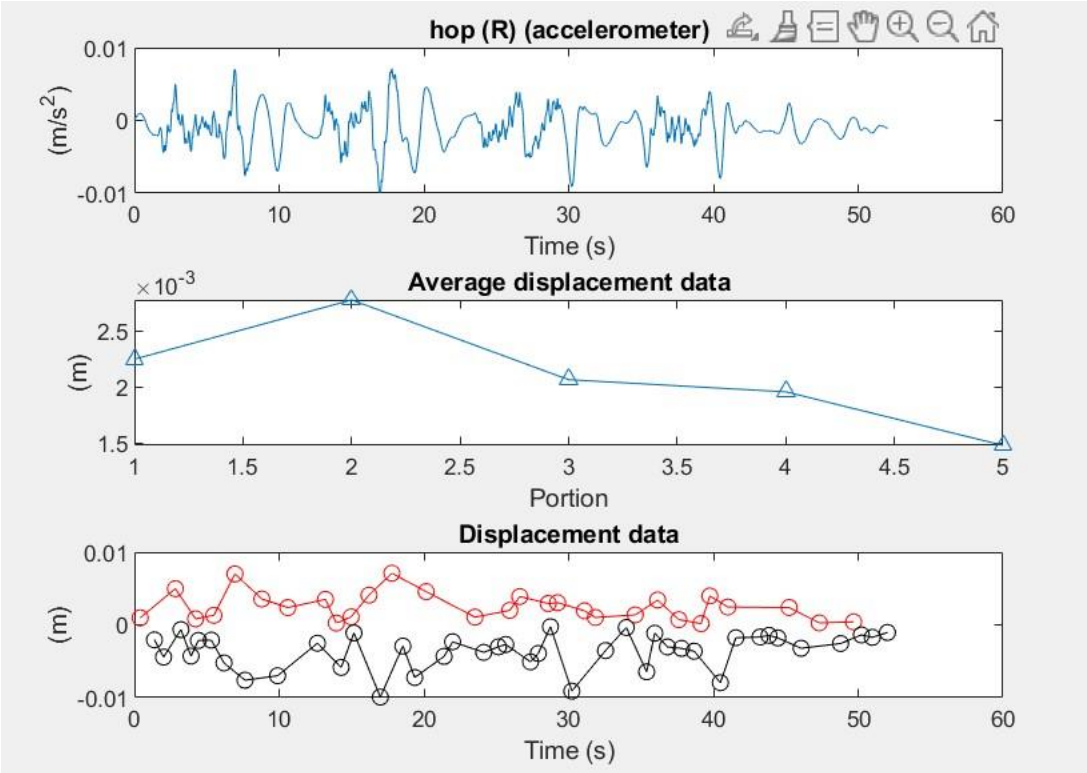

Figure 8: Hop (R) data

Figure 8 summarizes data for right hop data as recorded by the IMU. The activity is depicted in Figure 7. It focuses on the wearer's hop (R) acceleration, the average displacement data, and the displacement data. All the measurements are computed from the Y axis. There is a slight difference in displacement occasioned by the right hop compared to the left hope. For instance, a comparison of the average displacement data in Figure 6 and 8 show that while an increase in acceleration consistently increased and decreased displacements left and right from the Y axis in Figure 6, it consistently decreased when the IMU wearer hopped on the right leg. As a result, Figure 8 confirms that an increase in acceleration when hopping on the right leg decreases displacement from the Y axis. However, both right and left hops differ from normal walking, which informed an increase in average displacement whenever there was increased acceleration.

3.1.1.5 Jog:

Figure 9: Jog test

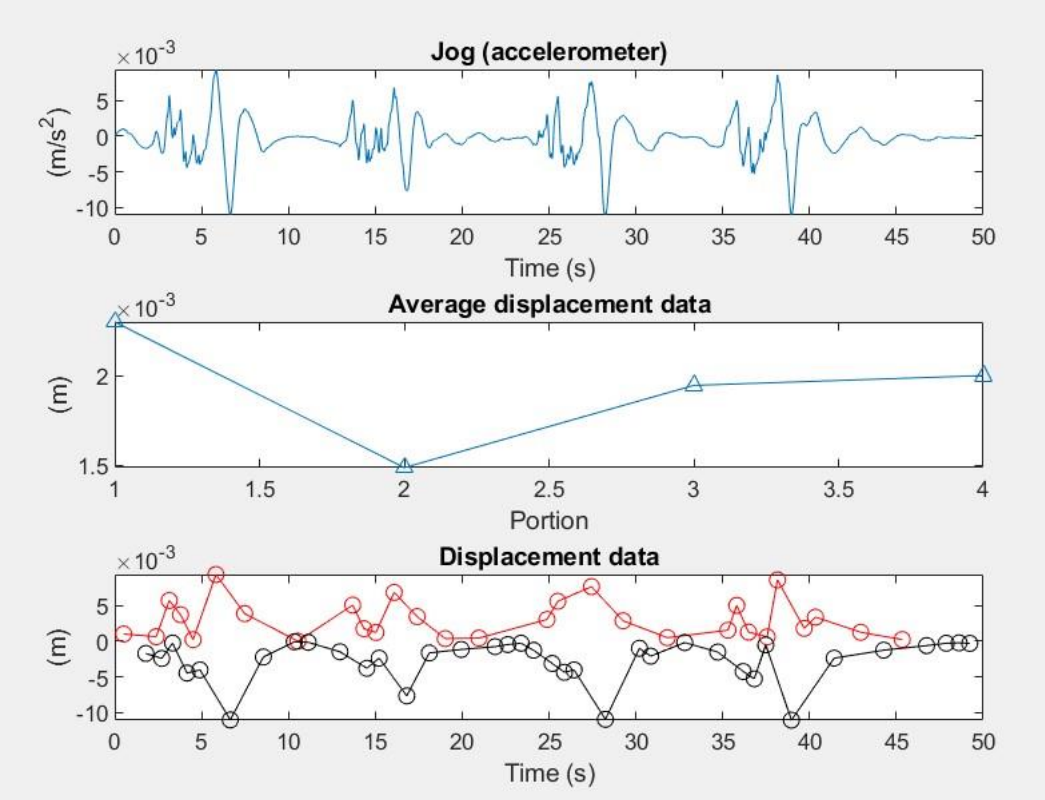

Figure 10: Jog data

Figure 10 summarises the jog data recorded by the IMU. The activity is depicted in Figure 9. It focuses on the jog acceleration in m/s, the average displacement data, and the displacement data during the activity. At the onset of the jog, there is a sharp increase in the right and left movements in the first 5 to 10 seconds. Increased acceleration then informs a drop in the average displacement before the rise in displacement at 30 seconds. It however stabilizes in the subsequent minutes of jogging. The trend differs from all the other preceding tests conducted.

3.1.1.6 Comparing data:

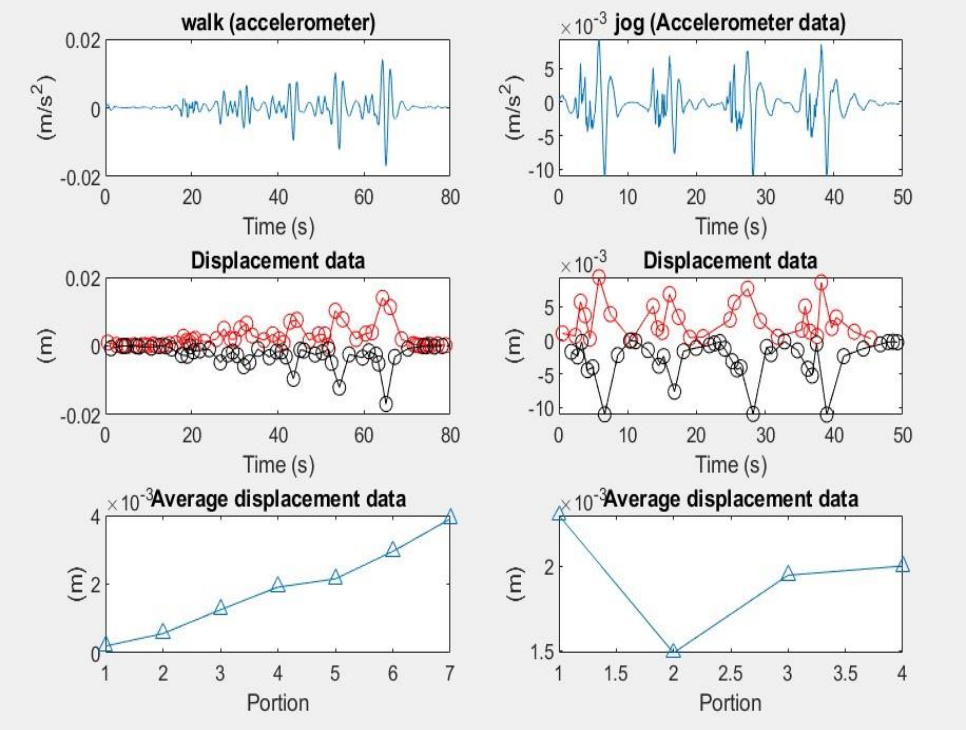

Figure 11: Comparing between normal Walk and Jog data

Figure 11 compares between normal walk and jog data. From the data trends it is evident that the Y axis go right and left. The normal walk graph indicates that it displacement increases consistently with the increase in acceleration. In jogging however, there is high displacement at the onset of the activity. However, with increased acceleration, there is a sharp decrease in displacement followed by another sharp increase in displacement. The increase is succeeded with stability in the displacement.

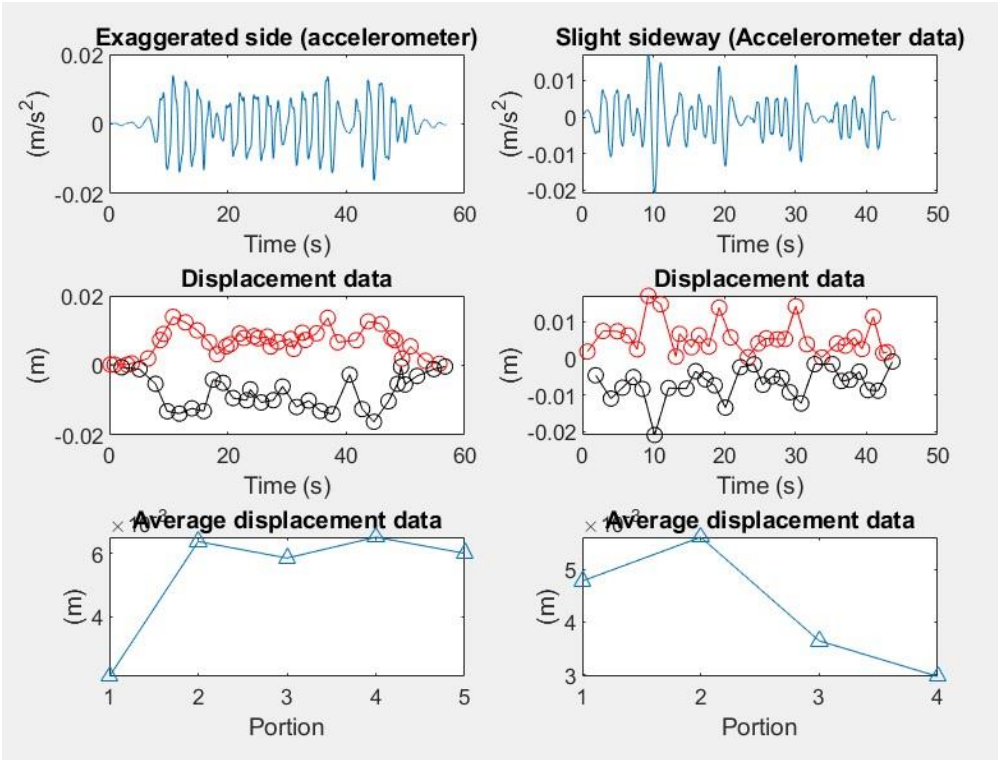

Figure 12: Comparing between Exaggerated side and Slight sideway data

Figure 12 represents the exaggerated side and slight sideway data obtained from the IMU. The average displacement data sharply rises in the exaggerated side to stabilize with the increase in acceleration. However, in the slight sideway data, average displacement first rises by consistently drops with the increase in acceleration. It is based on this observation that Y axis is the focus of this thesis.

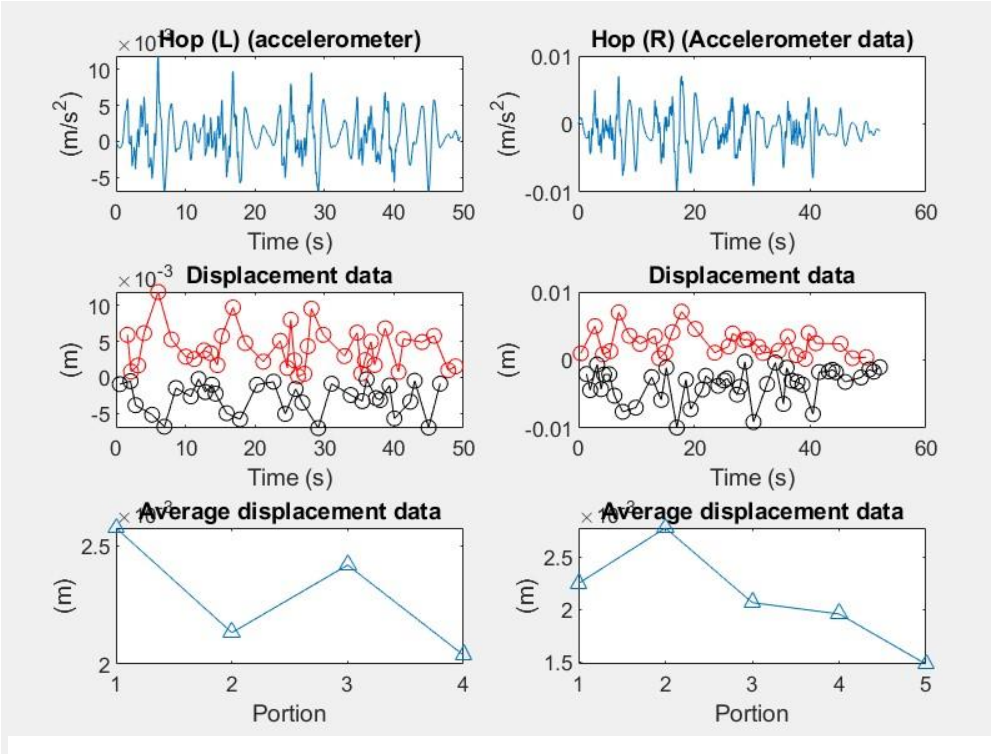

Figure 13: Comparing between Hop (L) and Hop (R) data

Figure 13 is comparing between Hop (L) and Hop (R) data and shown that X axis is up and down. There is a slight difference in displacement occasioned by the right hop compared to the left hope. For instance, a comparison of the average displacement data in left hop and right hop shows that while an increase in acceleration consistently increased and decreased displacements right and left on the left hop, it consistently decreased when the IMU wearer hopped on the right leg.

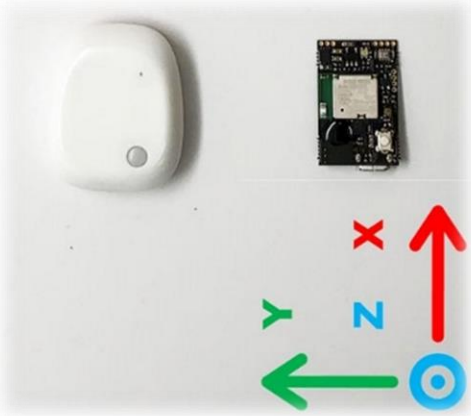

Figure 14: IMU direction position.

3.2 Description of the accelerometer output and displacement computation

"Specific force" ($\boldsymbol{a}$) is the difference between the body's acceleration ($\boldsymbol{a}_{body}$) and a gravity acceleration ($\boldsymbol{g}$). The sensor's local coordinate system (LCS) resolves all quantities, and the results are summarised in (1):

$$\boldsymbol{a} = (\boldsymbol{a}_{body} - \boldsymbol{g}) \tag{1}$$

From (1), it is possible to understand that when the MIMU is moving, the contribution of the $\boldsymbol{a}_{body}$ term is superimposed with $\boldsymbol{g}$ and the two terms cannot be distinguished unless an additional source of information is used. Typically, the orientation of the unit (${}^{GCS}R_{LCS}$) is estimated using a sensor fusion algorithm concerning a global coordinate system (GCS), Gravity is aligned vertically and one horizontal axis (often x-axis) points in a direction specified by Earth's magnetic north projected onto horizontal plane. (Caruso et al., 2021), as represented in Figure 15.

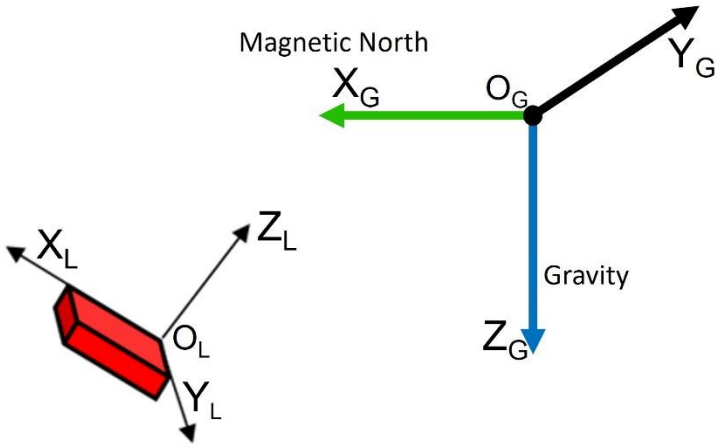

Figure 15: orientation of the sensor LCS with respect to the GCS.

A sensor fusion architecture is used to calculate ${}^{GCS}R_{LCS}$ using the complimentary properties of the accelerometer, gyroscope, and magnetometer data (Sabatini, 2011). Once ${}^{GCS}R_{LCS}$ is computed, the gravity vector is removed from the accelerometer readings as follows:

$$\boldsymbol{a}_{body} = \boldsymbol{a} + {}^{GCS}R'_{LCS}\,{}^{GCS}\boldsymbol{g} \tag{2}$$

After that, the three-dimensional displacement $\boldsymbol{d}$ is computed by double integrating the $\boldsymbol{a}_{body}$ term.

$$\boldsymbol{d} = \int_{t_1}^{t_2} \int_{t_1}^{t_2} \boldsymbol{a}_{body}\ dt \tag{3}$$

Where t_1 and t_2 corresponded to the first and last sample, respectively. It is clear that the initial conditions on the velocity should be provided for the first-time integration to obtain meaningful $\boldsymbol{d}$ values. Typically, t_1 and t_2 are selected to match the instants corresponding to null velocity (i.e., the body is still in both t_1 and t_2). By doing so, the initial velocity conditions can be set equal to zero.

3.3 Assumptions

It can be assumed that the accelerometer is perfectly fixed on the pelvis surface so that its vertical axis is coincident with the gravity vector direction when the subject is standing still. In this case, the two horizontal axes would sense a null gravity contribution, thus no longer requiring the estimation of ${}^{GCS}R_{LCS}$. In particular, the accelerometer axis aligned along the mediolateral direction of the body is the one of interest to compute the sway. Obviously, this assumption is weak due to the impossibility of a perfect position of the sensor due to the body's rounded surfaces, as depicted in Figure 16 (Benedetti et al., 2017; Cereatti et al., 2015).

Figure 16: The positioning of the accelerometer on the lower back. The sensor's actual LCS is highlighted in black, while the target LCS is represented with dashed green lines.

To overcome this limitation, a virtual realignment was performed as the sensor was positioned perfectly vertical to have the x-axis vertical and the y-axis horizontal during the standing position (Caruso et al., 2020; Zedda et al., 2020). The latter was identified as follows and graphically represented in Figure 17.

The accelerometer norm was computed for each timestamp:

$$a_{norm} = \sqrt{a_x^2 + a_y^2 + a_z^2}$$

- The mean value of a_{norm} was subtracted.
- The standard deviation was computed using a moving window of 25 samples (250 ms) for the first 15 seconds of each recording.
- The indexes of the samples correspond to a value of a_{norm} lower than 0.01 m/s^2 were identified.
- The continuous longest sequence of samples identified at the previous point was selected to represent the standing part.

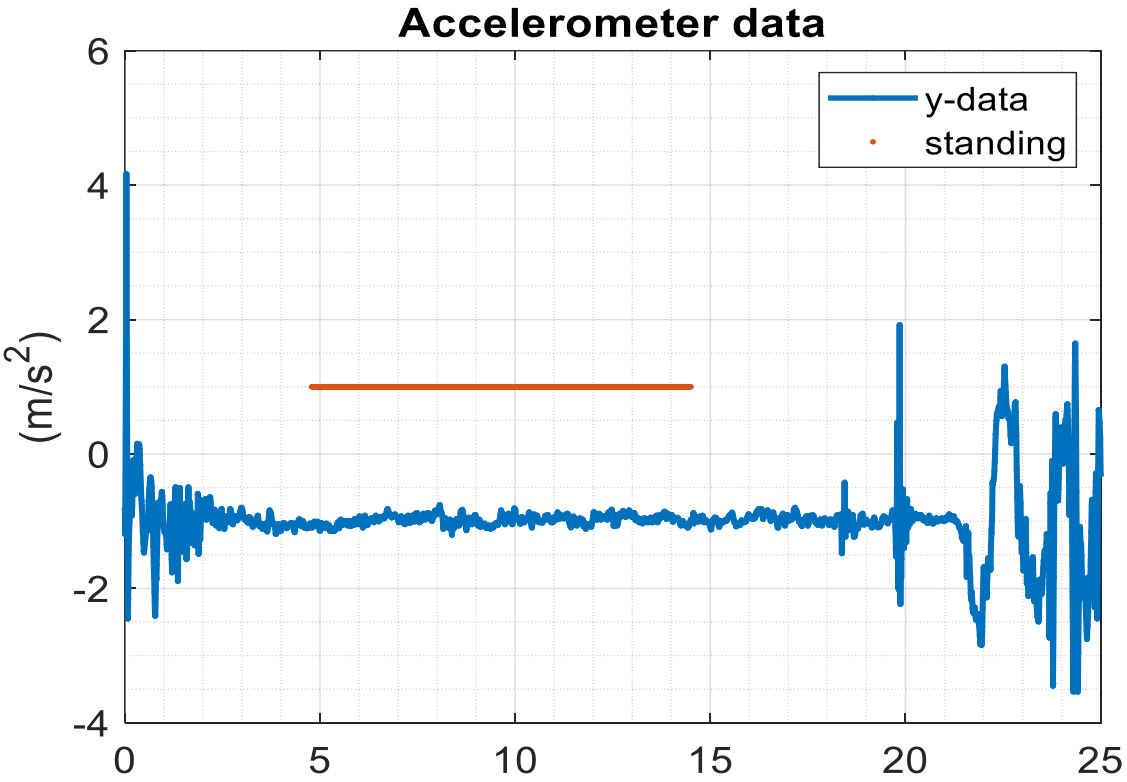

Figure 17: the standing part is identified by the orange horizontal line.

In the standing part, the following procedure was performed to compute the realignment matrix R_{meas}^{vert} which is defined by an angular rotation $\Delta\theta$ around a rotation axis k. The matrix was computed by comparing the measured accelerometer signals $\boldsymbol{a_{meas}} = [a_x, a_y, a_z]\frac{m}{s^2}$ with those which were measured if the accelerometer was perfectly vertical $\boldsymbol{a_{id}} = [9.81,\ 0,\ 0]\frac{m}{s^2}$ following an approach similar to that described in (Vitali et al., 2017):

- $\Delta\theta = \text{acos}\left(\frac{\boldsymbol{a_{id}}}{|\boldsymbol{a_{id}}|} \cdot \frac{\boldsymbol{a_{meas}}}{|\boldsymbol{a_{meas}}|}\right)$Where the $\cdot$ operator means the scalar product.

- $k = \left(\frac{\boldsymbol{a_{id}}}{|\boldsymbol{a_{id}}|} \wedge \frac{\boldsymbol{a_{meas}}}{|\boldsymbol{a_{meas}}|}\right)$Where the ∧ operator means the vector product.
- R_{meas}^{vert} was finally obtained using the Euler-Rodrigues's formula (Murray et al., 2017):

$$R_{meas}^{vert} = \boldsymbol{I} + \sin(\Delta\theta)\,\boldsymbol{K} + (1 - \cos(\Delta\theta))\boldsymbol{K}^2 \quad (4)$$

where $\boldsymbol{K}$ is the skew-symmetric form of the axis k:

$$\boldsymbol{K} = \begin{bmatrix} 0 & -k_z & k_y \\ k_z & 0 & -k_x \\ -k_y & k_x & 0 \end{bmatrix} \quad (5)$$

The last step of the realignment procedure consisted of the rotation of the measured signal onto the new vertical coordinate system:

$$\boldsymbol{a_{vert}} = R_{meas}^{vert} * \boldsymbol{a_{meas}} \quad (6)$$

From this point on, only the y-axis (i.e., medio-lateral direction) of the new rotated a_{vert} was considered.

3.4 Overview of the data processing pipeline

The data processing pipeline is reported in Figure 18. All these steps were implemented using MATLAB R2021a (The MathWorks Inc., Natick, MA, USA).

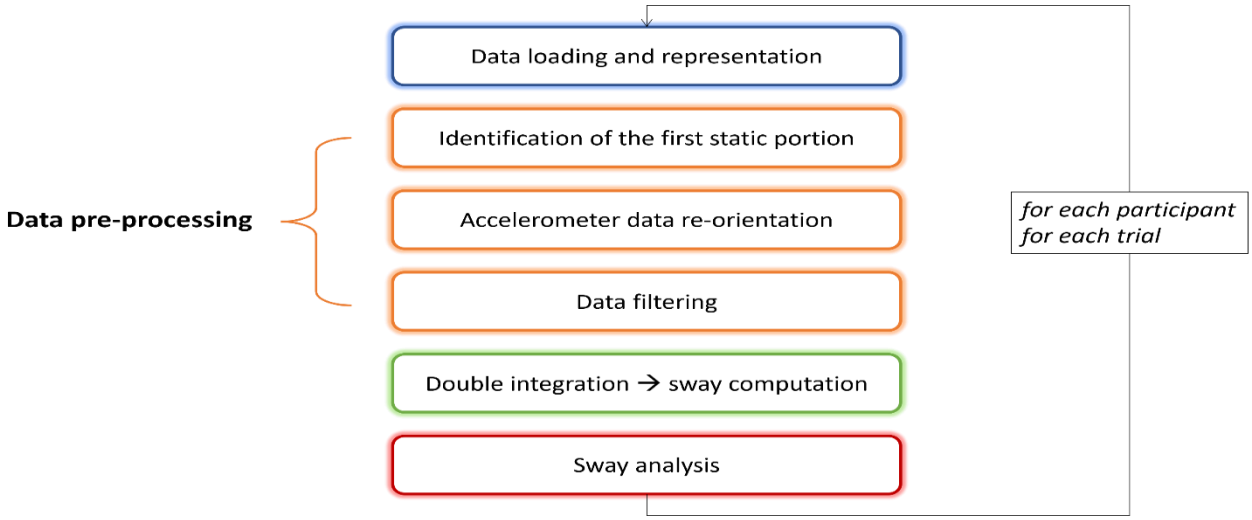

Figure 18: pipeline for the data processing. These steps were repeated for each participant and for each trial.

3.5 Data pre-processing and sway computation

After having imported the accelerometer data in MATLAB, the realignment processing described above is implemented to obtain $\boldsymbol{a_{vert}}$. The y-axis time-series were high-pass filtered using a 6th order Butterworth filter to limit the slow-changing variation of the accelerometer offset (Hussen & Jleta, 2015). At the end of this stage the $\boldsymbol{a_{vert_f}}$ was obtained. The cut-off frequency was set at 100 mHz. The mask of the filter in terms of both magnitude and phase is reported in Figure 19.

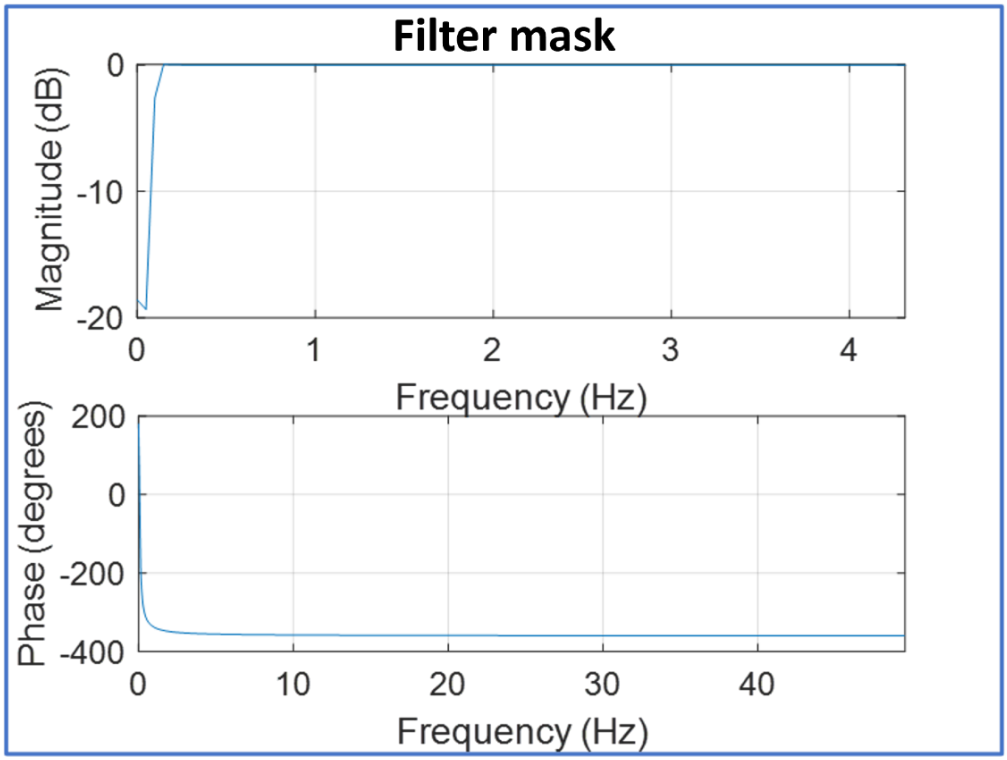

Figure 19: Mask of the high-pass filter

However, due to the non-idealist of both the filter and the calibration model, the filtered data had a (little) residual in the mean, which was then removed. This was done to avoid a drift growing unbounded overtime when double-integrating the acceleration. The mean value (indicated with $\boldsymbol{b_{vert_f}}$) when integrated results in a line whose value is proportional to the elapsed time:

$$\int_{t_1}^{t_2}\int_{t_1}^{t_2}(\boldsymbol{a_{vert_f}} + \boldsymbol{b_{vert_f}})\,dt = \tag{7}$$

$$\int_{t_1}^{t_2} (\boldsymbol{v}_{\boldsymbol{vert_f}} + \boldsymbol{b}_{\boldsymbol{vert_f}} (t_2 - t_1))\, dt =$$

$$\boldsymbol{d}_{\boldsymbol{vert_f}} + \frac{1}{2} \boldsymbol{b}_{\boldsymbol{vert_f}} (t_2 - t_1)^2$$

The first term represents the sway (which has zero mean), while the second $\frac{1}{2} \boldsymbol{b}_{\boldsymbol{vert_f}} (t_2 - t_1)^2$ represents the errors due to the mean value caused by the non-idealist of the filter and the calibration model. For example, the gravity value was assumed to be equal to 9.81 $\frac{m}{s^2}$ but actual measurements may differ from this value depending on the accuracy of the implemented calibration model (Parvis & Ferraris, 1995; Stančin & Tomažič, 2014). To sum up, the subtraction of the mean value was a simple strategy to mitigate the non-idealist of the pre-processed data. This operation was possible since the velocity at the beginning and the end was null (i.e., velocity mean value equal to zero). By having removed the mean value only, it is possible to assume that the sway is represented by $\boldsymbol{d}_{\boldsymbol{vert_f}}$.

3.6 Sway analysis

For each patient and each of the two trials, the analysis of the $\boldsymbol{d}_{\boldsymbol{vert_f}}$ characteristics were performed separately for 12 portions of the signal since the experimental protocol involved 12 repetitions at an increasing walking speed. For each signal portion, the positive and negative peaks of $\boldsymbol{d}$ were identified as metrics of oscillation of the lower back at each gait cycle (Kamen et al., 1998; Mancini et al., 2012). The displacement and average displacement data assisted in computing the differences between the two trials.

Thus, the amplitude of the sway was computed as follows:

$$A_{sway} = \max\left(\boldsymbol{d}_{\boldsymbol{vert_f}}\right) - \min\left(\boldsymbol{d}_{\boldsymbol{vert_f}}\right) \quad (8)$$

The maxima and minima are reported in Fuger 20 and Figure 21.

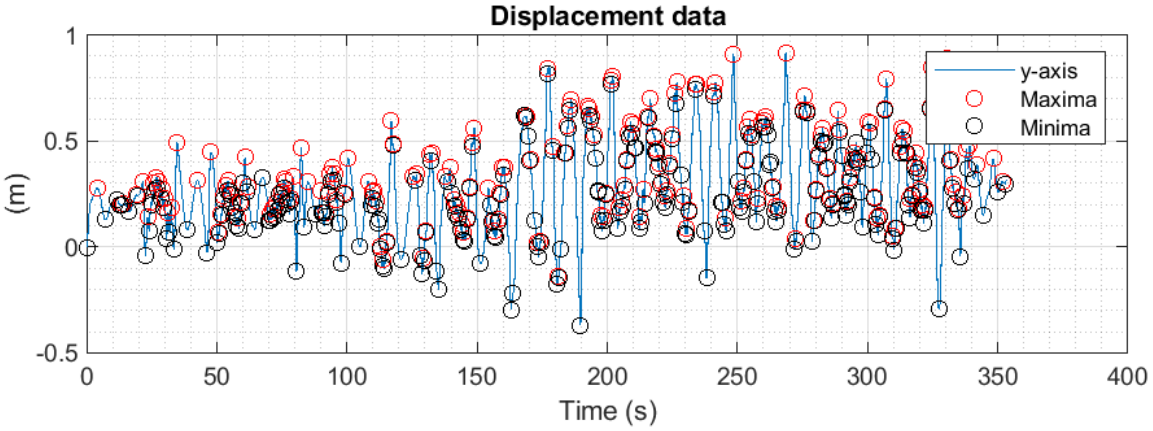

Figure 20: Trial 1, the time-series of d_{vert_f}. Data are referred to subject #1, as an example.

Figure 20 summarises the minimum and maximum displacement data. At the onset of the movement, there is a low displacement from the y-axis. However, an increase in acceleration consistently increases the displacements. For instance, the displacements recorded between 150 and 350 seconds are much higher compared to those recorded between 0 and 150 seconds.

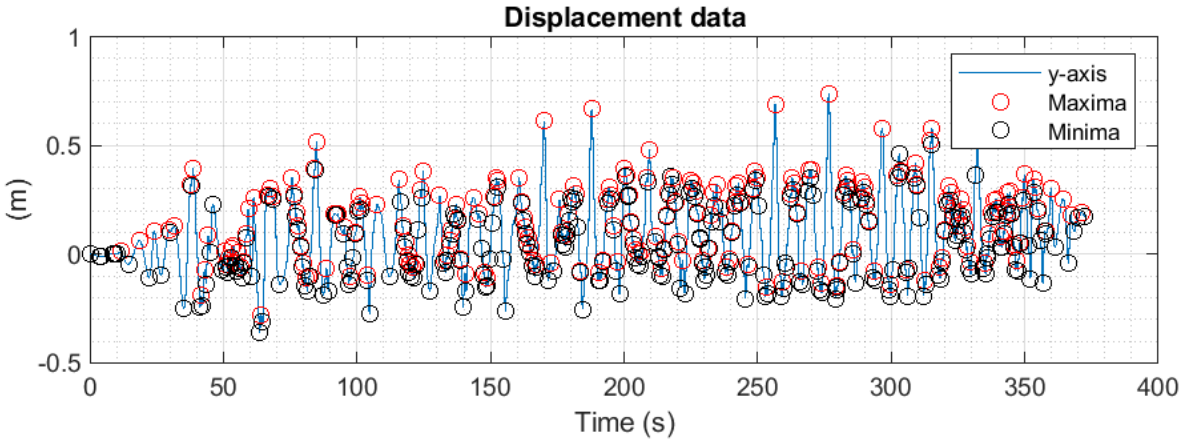

Figure 21: Trial 2, the time-series of d_{vert_f}. Data are referred to as subject #1 after effect by fatigue, as an example.

Figure 21 summarizes the effect of fatigue on displacement from the y-axis—increased acceleration when under fatigue equally increases the displacement consistently. For instance, acceleration between 0 and 150 seconds is lower than an acceleration between 150 and 300. The displacements, however, decrease upon reaching 300 seconds. The difference with Figure 20 is that the displacements are more sway to right and left.

The A_{sway} was then averaged for each portion to quantify the mean amplitude of the sway, thus obtaining 12 values, represented in Figure 22 and Figure 23.

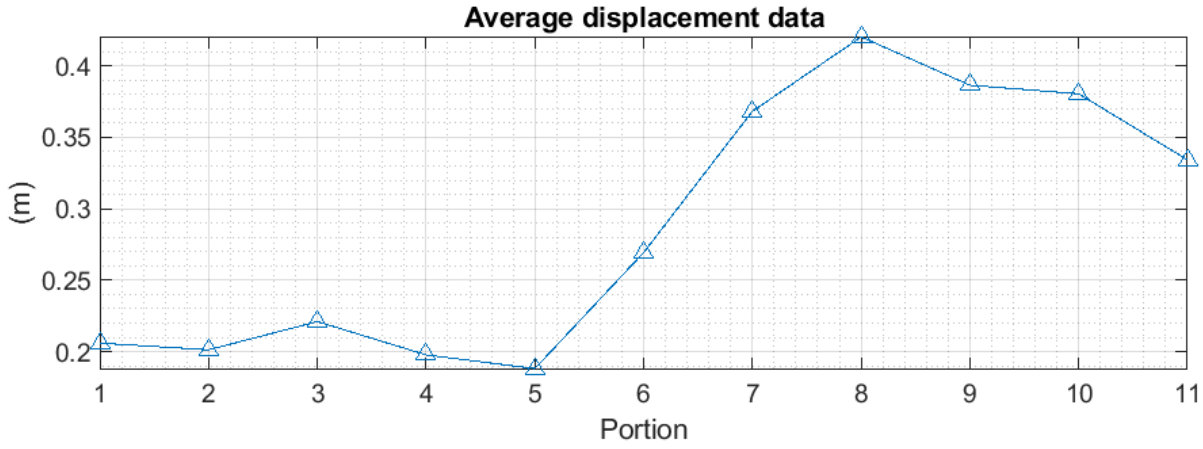

Figure 22: Trial 1, the 12 values representing the average A_{sway} for each of the 12 portions.

Figure 22 summarises the average displacement data for each of the 12 portions before effect by fatigue. At the onset, there is inconsistency in the displacement with a decrease between the first two values. There is then an increase in displacement between portions two and three, followed by a reduction in displacement between 3 and 5. However, there is a consistent increase in displacement between portions 5 and 8 and that giving indcate the sway in here will be high.

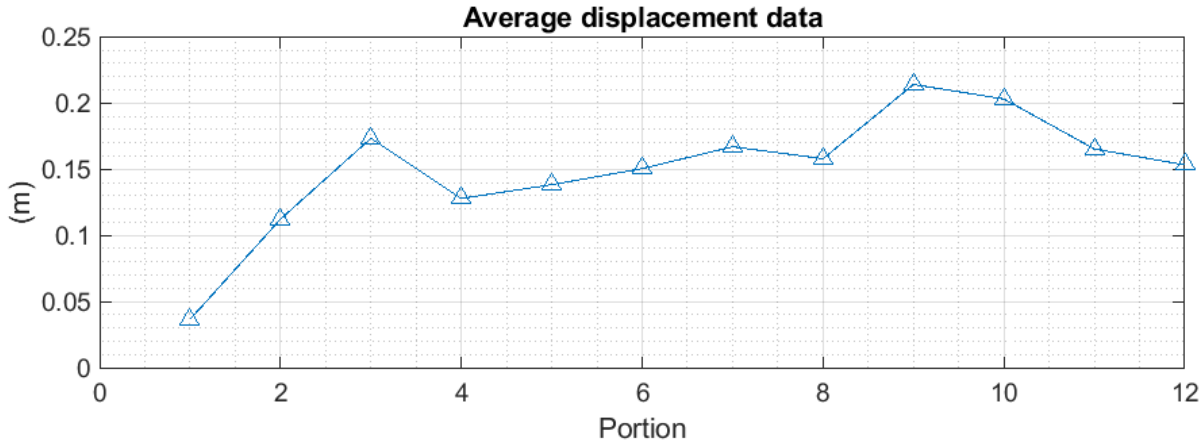

Figure 23: Trial 2, the 12 values representing the average A_{sway} after effect by fatigue for each of the 12 portions.

Finally, the difference between the average A_{sway} for the last and the first portions was computed. A positive value means that the amplitude increased with the increase of the walking speed. On the contrary, a negative value means that the amplitude decreases with the decrease of the walking speed. This entire process was repeated for each of the two trials and for each subject.

4. RESULTS

The differences between the average A_{sway} for the last and the first portions are reported in Table I.

Amplitude difference	***First trial (cm)***	***Second trial (cm)***	***Age***	***Gender***
Subj #1	12	5	73	F
Subj #2	-7	-40	57	M
Subj #3	-2	-3	68	F
Subj #4	5	7	56	M
Subj #5	12	32	69	F
Subj #6	-2	-5	58	F
Subj #7	-14	-13	44	F
Subj #8	2	-2	65	M
STD	9.0	20.2		

From table above, it is possible to observe that the results were variable depending on the subject and on the single-trial (STD equal to 9 cm and 20 cm, respectively). However, the trend was similar for all the participants in terms of increasing or decreasing the amplitude between the two trials, i.e., the sign of the difference remained constant. An exception was represented by the last subject, but this could be explained by the fact that the differences were almost null. Half of the subjects exhibited a sway amplitude increase. Overall, the difference in the amplitude was below

15cm, but for the second trials of subjects 2 and 5 which values amounted to -40 cm and 32 cm, respectively.

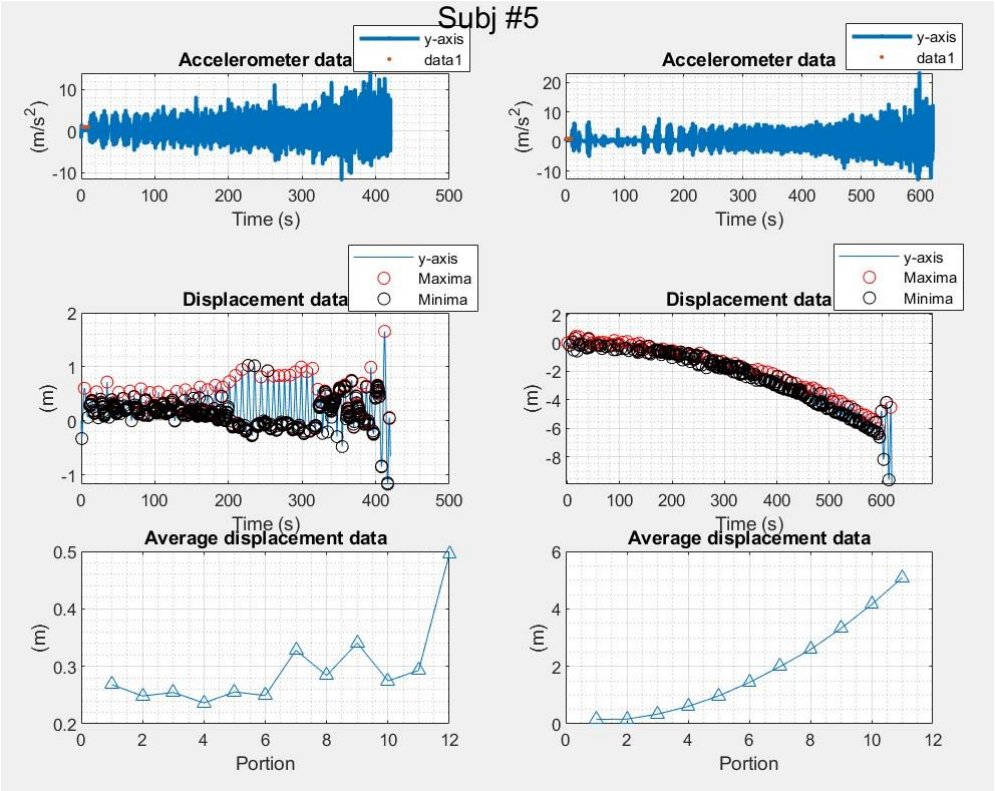

Figure 24 : Trials 1 and 2 for Subject #5

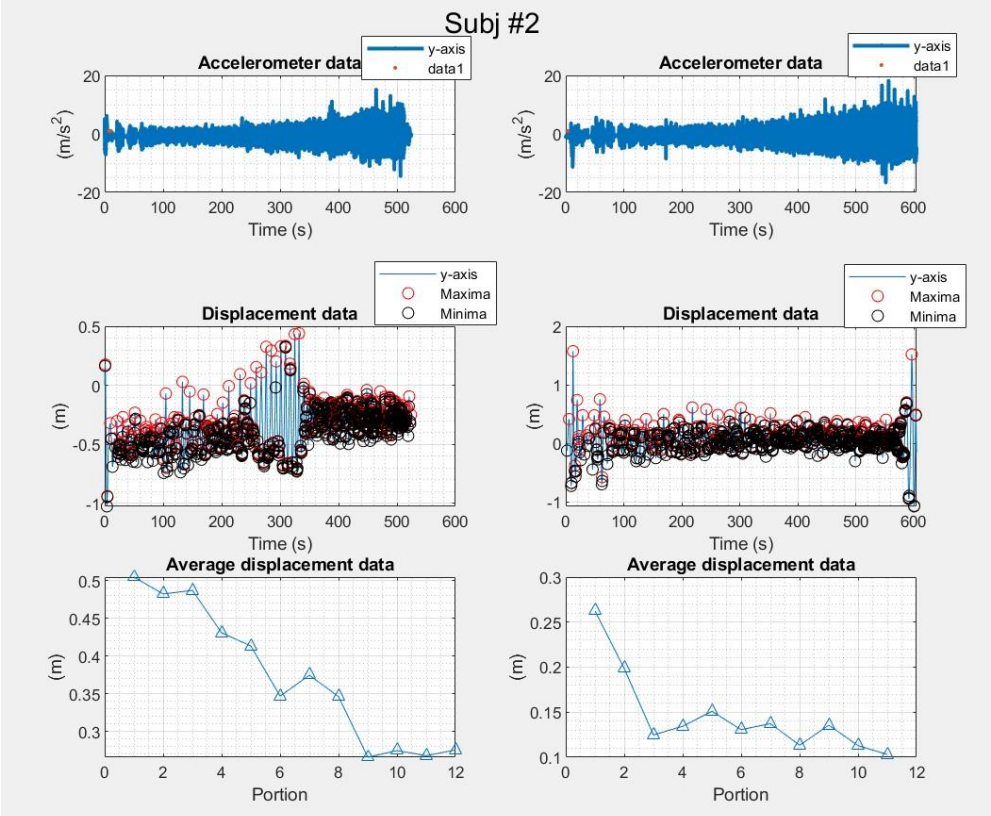

Figure 25 :Trials 1 and 2 for Subject #2

In this case, Subject 5 show above in Figure 24 first trail was stable and average sway is 12cm but in second trial was big sway about 32cm (20 cm different gap) from first trial (Result from table I) and that giving indicate this subject #5 was affected by fatigue more than other participants specially when her age 69 old. However, in subj2 same thing was happen different gap between first and second trials about 33cm and that not usually normal specially when his age 57 old. So, as Figure 25 show for second trial displacement data there is big sway in begging and end of test and that could be prepare to start test and doing some stretch by the end. IMU can predict the risk of falling during walking and standing.

5. DISCUSSION

For the process involved in the measurement or assessment of the sensors or the placement of the sensors or its positions, no fixed or consistent number is recommended or considered appropriate or needed. Regardless, from several reviewed studies, the preferred location or site was within the lumbar spine (L3-L5). It is understandable from the reviewed studies that a single inertial sensor in terms of reliability is the same as using the multiple inertial sensors once the position during measurement is done appropriately, as in placement on the center of mass (L3-L5) (Ghislieri et al. 2019). At this point, while recording the data, analysis is bound to give moderate to good Validity during the test for reliability of the static and dynamic balance (Baker et al. 2021). In clinical settings, using a single sensor placed at the region of the center of mass makes it easier for the clinician to observe the required data, especially during the telehealth interactions concerning the needed instructions, observations, and interventions with the devices targeted at providing. Researchers have utilized single sensors to identify the major differences that exist between the fallers and non-fallers. This (the use of a single inertial wearable sensor) appears to be pertinent in this study because of the nature of the study, which relates sway analysis that is relevant to getting the important results. One of the issues that have made it essential is that multiple sensors have been shown to be common, which creates a state of an increased error because of the various positions each of the sensors reads its data from, making it compute different data. It is observable that the use of different placements for the wearable devices for both the static and dynamic balance activities and their respective body positions creates different challenges or issues with the pool of data collected (Baker et al. 2021). It is important to note that studies with different research questions demand different research analyses to solve the issue. Regardless of such difference in analysis, there is a need to have a standardized sensor positioning that will allow cross-comparison of results of studies to enable justification of recommendations. Increasing our understanding or knowledge of fall risk assessment makes it possible to have a consistent or gold standard requiring the placement of the equipment for measuring the various direction (ML and AP sway) during various moves, as in the static balance or step time, step length, and gait velocity for the dynamic balance. One issue that has created the different need for more studies remains the accuracy of the discrimination between healthy individuals and those diagnosed with certain health conditions. However, those sensors can still help discriminate between the young from those that are old or fallers from the non-fallers. Data used by studies differ some used accelerometer-related data, while some other devices included gyroscope and magnetometer data. This reduced the system's complexity, making it less difficult for clinicians noted to be less familiar with the technicalities of the new sensors or what is needed to integrate sensors into their clinical evaluation process.

Description of the wearable sensor placements during the methodology or experimental placement for each postural sway is fully done, attaching it to the subjects utilizing the elastic belts. For the sway computation, the accelerometer axis remains vital and made to be aligned along the ML direction of the body (Alvarez et al. 2018). However, because of weak assumptions created by the impossibilities that are associated with the existence of having a perfect positioning for the wearable sensor because the area it is usually placed in the body has a rounded surface, we tend to have the actual orientation and ideal orientation for the positioning of the accelerometer on the lower back. For the balance stance measurement, the subject is made to maintain their double leg stance for half a minute because of the effect studies have shown such to heavily had on the postural sway by helping to modify the base of the support. Feet positions in double leg stance come in various forms, such as feet opening angle, which ranges from 10-30 degrees, or self-selected feet position. As simple as the positioning appears, getting this in subjects is usually challenging, especially for those that suffer the problems with the balance-related disabilities. In most situations, patients prefer to keep their feet apart to ensure they are able to maintain balance, which gives them that ecological test condition that could be close to the real-life upright stance.

In this context, the mediolateral sway velocity during the walking represents the main parameter that helps differentiates those considered to be recurrent fallers from non-recurrent fallers. This is independent of the testing condition. When recorded data present with higher index values compared to the normative values, such can thus be considered to be suggestive of postural control deficit, especially those common with geriatric individuals with health disorders. In the recorded data for the two trials, the analysis output has shown the two sides of positive and negative with respective walking speeds placed. It is important for health professionals interested in utilizing such variables as a pointer to conduct other assessments further when they are already shown the likelihood of postural control deficit. Areas to also look after include the fall history, fear or use of medication, presence of issues with lower limb strength, and problems with proprioception or vestibular deficiencies. Suppose they have been recommended previous strategies to prevent falls or reduce chances of having injuries. Nevertheless, several postural sway parameters or features measured or extracted from the centre of pressure data were related to high fall risk. Those features have a way of helping to discriminate between those that are fallers and non-fallers. IMUs can be used to detect and quantify human movement factors that influence stability during ISWT.

5.1 Limitations

Despite the rigorous methodology developed to estimate the sway amplitude, some limitations must be underlined.

First of all, the accelerometer non-idealist may strongly contribute to the magnitude of the errors (Luinge & Veltink 2004). In fact, it is clear from (1) that the $\boldsymbol{a}_{body}$ contribution is zero when no accelerations are occuring, and the accelerometer function as an inclinometer simply by monitoring the gravitational tilt. In contrast, the accelerometer's $\boldsymbol{a}_{body}$ term is equal to $\boldsymbol{g}$ when it is in free fall, and the accelerometer's output is null. It is hard to accurately estimate the accelerometer inclination without other sources of information while the MIMU is moving because the $\boldsymbol{a}_{body}$ term is overlaid with $\boldsymbol{g}$. In addition, the measured accelerometer output a is corrupted by errors who's modelling commonly includes a matrix of scale factor error coefficients ($\boldsymbol{S}_a$), matrix of cross coupling error coefficients, also known as non-orthogonality ($\boldsymbol{M}_a$), a vector a of bias error ($\boldsymbol{b}_a$) and the vector representing its fluctuations ($\boldsymbol{\delta b}_a$), and white Gaussian noise as stated in equation (9) (Aydemir & Saranli, 2012; Unsal & Demirbas, 2012):

$$\boldsymbol{a} = (\boldsymbol{S}_a + \boldsymbol{M}_a)\big(\boldsymbol{a}_{body} - \boldsymbol{g}\big) + \boldsymbol{b}_a + \boldsymbol{\delta b}_a + \boldsymbol{w}_a \tag{9}$$

Specifically, $\boldsymbol{S}_a$ is the diagonal 3x3 matrix of coefficients expressing, for each axis, the deviation from ideal sensor sensitivity. This error typically consists of a constant component and temperature-induced variance. $\boldsymbol{M}_a$ represents the 3x3 matrix of the non-orthogonality errors between the three accelerometer sensing axes caused by the mechanical components' positioning. According to the trigonometric formula, the non-orthogonality causes an undesirable coupling of the axis' outputs. The axis output in the absence of g is represented by the $\boldsymbol{b}_a$ 3x1 vector, which is the accelerometer bias. The bias vector $\boldsymbol{b}_a$ contains a fixed part and temperature-induced variation. A calibration refinement method can adjust $\boldsymbol{S}_a$, $\boldsymbol{M}_a$, and $\boldsymbol{b}_a$ (Aslan & Saranli 2008). However, there are run-to-run variances, turn-on-to-turn-on variations, and a moderate shift over time in the bias error. The $\boldsymbol{\delta b}_a$ 3x1 vector reflects the latter components of the errors, which is one of the biggest issues when determining the displacement since the accelerometer data is doubly integrated after gravity reduction. A 3x1 vector of white Gaussian noise with zero mean $\boldsymbol{w}_a$ is the final result as part of the stochastic error components, the $\boldsymbol{\delta b}_a$and $\boldsymbol{w}_a$ vectors are only able to be statistically described (Ash et al. 1998; Systems et al. 2014).

The second limitation is represented by the fact that, despite the mathematical realignment, the hypothesis of a complete horizontality of the $\boldsymbol{a_{vert}}$ the y-axis (aligned along the mediolateral direction) may no longer hold during walking, depending on the subject-specific oscillation amplitude (Bolink et al. 2016). In fact, during gait, the y-axis of the accelerometer varied its orientation, thus sensing the relevant gravity vector projection. By assuming a perfectly sinusoidal oscillation, a model of the error is presented below:

$$\int_{t_1}^{t_2}\int_{t_1}^{t_2}(\boldsymbol{a_{vert_f}} + Asin(2\pi f_0 t))\,dt =$$

$$\int_{t_1}^{t_2}(\boldsymbol{v_{vert_f}} - 2\pi f_0 Acos(2\pi f_0 t))\,dt = \tag{10}$$

$$\boldsymbol{d_{vert_f}} - (2\pi f_0 A)^2\left(sin(2\pi f_0 t_2) - sin(2\pi f_0 t_1)\right)$$

In (10) the f_0 is the frequency of the oscillation, which is directly linked with the gait cycle frequency. As highlighted in the equation mentioned above, the amplitude of the errors is proportional to the square of the oscillation amplitude, and on f_0.

The last limitation is the sliding movement's soft tissue artifact, which causes a time-varying relative orientation between the IMU and pelvis axes (Berner et al. 2020). This issue may strongly contribute to increasing errors during the double integration process.

6. CONCLUSION

To sum up the current findings, wearable inertial devices have proven to be of great importance in differentiating between fallers and non-fallers. Despite having several limitations or unclear features relating to the measurements, continuous study and measurement have shown a better understanding of what needs to be measured or targeted while using IMUs or different forms of wearable devices. This study has enlightened what positive or negative amplitude of postural sway represents during increasing walking in terms of accuracy and validity. IMUs can be used to detect and quantify human movement factors that influence stability during incremental shuttle walk test (ISWT). Health care professionals and sports professionals can benefit from the proper understanding of postural sway amplitude as the determinant of individual key balance determinants. This can be used as a guide while evaluating their patients or athletes or planning their efficient rehabilitation programs that will help reduce the fall risk or prevent falls.

6.1 RECOMMENDATIONS

There are a number of recommendations that can be made. Wearable inertial devices that could easily be worn and achieve the actual orientation without errors need to be developed to reduce limitations in such areas, especially those related to errors during walking. There is also a need to see how different participants can be recruited.

6.2 FUTURE WORK

Further research is needed in several areas to evaluate the convergent validity required to use a single sensor to collect data over the centre of mass compared to those studies that used six sensors in clinical settings. Also, further research to use that single sensor to discriminate the postural sway differences between healthy and unhealthy individuals or between subjects with major age groups differences, or between those that could be classified as fallers or non-fallers in either clinical or natural settings.

7. BIBLIOGRAPHY

Alvarez, C, Álvarez, D & López, M 2018, 'Accelerometry-based distance estimation for ambulatory human motion analysis', *Sensors (Switzerland)*, vol. 18, no. 12, 4441-4461. doi: 10.3390/s18124441.

Ash, M, Morris, H, & Peters, R 1998 'Proposed IEEE accelerometer standard and other inertial sensor standards' *1998 Guidance, Navigation, and Control Conference and Exhibit,* 1322–1330. https://doi.org/10.2514/6.1998-4405

Aslan, G & Saranli, A 2008, 'Characterization and calibration of MEMS inertial measurement units'. *European Signal Processing Conference, Eusipco*.

Aydemir, G, & Saranli, A 2012 'Characterization and calibration of MEMS inertial sensors for state and parameter estimation applications' *Measurement: Journal of the International Measurement Confederation,* 45(5), 1210–1225. https://doi.org/10.1016/j.measurement.2012.01.015

Baker, N, Gough, C & Gordon, S 2021, 'Inertial sensor reliability and validity for static and dynamic balance in healthy adults: A systematic review', *Sensors*, 21(15), 5167-5182. doi: 10.3390/s21155167.

Benedetti et al. 2017 'SIAMOC position paper on gait analysis in clinical practice: General requirements, methods and appropriateness' *Results of an Italian consensus conference*. Gait and Posture, 58, 252–260. https://doi.org/10.1016/j.gaitpost.2017.08.003

Berner et al. 2020 'Concurrent validity and within-session reliability of gait kinematics measured using an inertial motion capture system with repeated calibration' *Journal of Bodywork and Movement Therapies,* 24(4), 251-260. https://doi.org/10.1016/J.JBMT.2020.06.008

Bolink et al. 2016 'Validity of an inertial measurement unit to assess pelvic orientation angles during gait, sit–stand transfers and step-up transfers: Comparison with an optoelectronic motion capture system' *Medical Engineering & Physics,* 38(3), 225–231.

https://doi.org/10.1016/J.MEDENGPHY.2015.11.009

Caruso et al. 2021 ‘Analysis of the Accuracy of Ten Algorithms for Orientation Estimation Using Inertial and Magnetic Sensing under Optimal Conditions: One Size Does Not Fit All’ *Sensors*, 21(7), 2543. https://doi.org/10.3390/s21072543

Caruso et al. 2021 ‘Real-Time Kinematics Estimation In Tele-Rehabilitation’. 2, 2058.https://www.researchgate.net/publication/353515186_Real-time_joint_kinematics_estimation_in_tele-rehabilitation

Cereatti, A, Trojaniello, D & Croce, U 2015 ‘Accurately measuring human movement using magneto-inertial sensors: Techniques and challenges’ *2nd IEEE International Symposium on Inertial Sensors and Systems*, IEEE ISISS 2015 - Proceedings, 1–4. https://doi.org/10.1109/ISISS.2015.7102390

Doheny, EP et al. 2012 'Displacement of centre of mass during quiet standing assessed using accelerometry in older fallers and non-fallers', *Proceedings of the Annual International Conference of the IEEE Engineering in Medicine and Biology Society*, EMBS, pp. 3300–3303.

doi: 10.1109/EMBC.2012.6346670.

Evans, A & Goldstein, S 2014, 'Pulmonary Rehabilitation', *Comprehensive Biomedical Physics*, vol. 10, pp. 411–422. doi: 10.1016/B978-0-444-53632-7.01027-3.

Ghislieri, et al. 2019, 'Wearable inertial sensors to assess standing balance: A systematic review. *Sensors*, vol. 19, no. 19, 4075.

Haagsma, A et al. 2020 'Falls in older aged adults in 22 European countries: incidence, mortality and burden of disease from 1990 to 2017', *Tuomo J Meretoja*, vol. 26, pp. 46 - 56.

doi: 10.1136/injuryprev-2019-043347.

Hubble, et al. 2015, 'Wearable sensor use for assessing standing balance and walking stability in people with Parkinson's disease: a systematic review' *PloS one*, vol. 10, no. 4, 1-22 e0123705.

Hussen, A & Jleta, I 2015 ‘Low-Cost Inertial Sensors Modeling Using Allan Variance’ *International Scholarly and Scientific Research & Innovation*, 9(5), 1069–1074.

Kamen, et al. 1998 ‘An Accelerometry-Based System for the Assessment of Balance and Postural Sway’ *Gerontology*, 44(1), 40–45. https://doi.org/10.1159/000021981

Luinge, H & Veltink, P 2004 ‘Inclination Measurement of Human Movement Using a 3-D Accelerometer with Autocalibration’. *IEEE Transactions on Neural Systems and Rehabilitation Engineering*, 12(1), 112–121. https://doi.org/10.1109/TNSRE.2003.822759

Mancini et al. 2012 ‘Postural sway as a marker of progression in Parkinson's disease: A pilot longitudinal study’ *Gait & Posture*, 36(3), 471–476. https://doi.org/10.1016/J.GAITPOST.2012.04.010

McAndrew P, Wilken, J & Dingwell, J 2012, 'Dynamic Margins of Stability During Human Walking in Destabilizing Environments, *J Biomech*, vol. 45, no. 6, pp. 1053–1059. doi: 10.1016/j.jbiomech.2011.12.027.

Mobbs et al. 2022, 'Gait metrics analysis utilizing single-point inertial measurement units: a systematic review' *Mhealth*, vol. 8. doi: 10.21037/mhealth-21-17

Murray, R & Shankar , S 2017 ‘A mathematical introduction to robotic manipulation’ *A Mathematical Introduction to Robotic Manipulation*, 1–456.

https://doi.org/10.1201/9781315136370/MATHEMATICAL-INTRODUCTION-ROBOTIC-MANIPULATION-RICHARD-MURRAY-ZEXIANG-LI-SHANKAR-SASTRY

Neville, C, Ludlow, C & Rieger, B 2015, 'Measuring postural stability with an inertial sensor: Validity and sensitivity', *Medical Devices: Evidence and Research*, vol. 8, pp. 447–455.

doi: 10.2147/MDER.S91719.

Pang et al. 2019, 'Detection of near falls using wearable devices: a systematic review' *Journal of geriatric physical therapy*, vol. 42, no. 1, pp. 48-56.

Parvis, M & Ferraris, F 1995 ‘Procedure for effortless in-field calibration of three-axial rate gyro and accelerometers’ *Sensors and Materials*, 7(5), 311–330.

Rantalainen et al. 2020, 'Gait variability using waist-and ankle-worn inertial measurement units in healthy older adults' *Sensors*, vol. 20, no. 10, 2858.

Sabatini, A 2011 ‘Estimating three-dimensional orientation of human body parts by inertial/magnetic sensing’ *Sensors*, 11(2), 1489–1525. https://doi.org/10.3390/s110201489

Stančin, S & Tomažič, S 2014 ‘Time- and computation-efficient calibration of MEMS 3D accelerometers and gyroscopes’ *Sensors (Switzerland)*, 14(8), 14885–14915. https://doi.org/10.3390/s140814885

Su, B, Smith, C & Gutierrez Farewik E 2020, 'Gait phase recognition using deep convolutional neural network with inertial measurement units' *Biosensors*, vol. 10, no. 9, pp. 109 – 119

Systems, M., Development, S., & Devices, E. (2014). IEEE Standard for Sensor Performance Parameter Definitions. In IEEE Standard. https://doi.org/10.1109/IEEESTD.2014.6880296

Szczegielniak et al. 2018, ‘A study on nonlinear estimation of submaximal effort tolerance based on the generalized MET concept and the 6MWT in pulmonary rehabilitation’ *PLoS One*, vol. 13, no. 2, pp. 1-18.

Unsal, D & Demirbas, K 2012 ‘Estimation of deterministic and stochastic IMU error parameters’ *Record - IEEE PLANS, Position Location and Navigation Symposium*, 862–868. https://doi.org/10.1109/PLANS.2012.6236828

Vitali et al. 2017 ‘Method for estimating three-dimensional knee rotations using two inertial measurement units: Validation with a coordinate measurement machine’. *Sensors (Switzerland)*, 17(9), 1970. https://doi.org/10.3390/s17091970

Zedda et al. 2020 ‘DoMoMEA: A Home-Based Telerehabilitation System for Stroke Patients/’. *Proceedings of the Annual International Conference of the IEEE Engineering in Medicine and Biology Society*, EMBS, 2020-July, 5773–5776. https://doi.org/10.1109/EMBC44109.2020.9175742

APPENDICES

```
%% Set up the Import Options and import the data
clearvars
clc
close all

% 1) IMPROVE THE READING OF THE DATA AND IMPLEMENT THE AUTOMATIC READING OF
% ALL THE FILES - OK

pathData = 'Data';
patients = 1:8;

sk = zeros(12,2,8);
rmsmaxmin = zeros(12,2,8);

for idx = patients

    figure
    for rep = 1:2
        %% Read data
        acc = readmatrix([pathData filesep 'iswt' num2str(idx) '(' num2str(rep) ').csv']);

        if (idx == 5 && rep == 1)
            acc = acc(200*100:end,:);
        elseif(idx == 7 && rep == 1)
            acc = acc(51*100:end,:);
        end

        t = acc(:,3);
        t = t - t(1);
        t = t - t(1);
        accy = acc(:,5)*9.81;

        N = size(t,1);

        subplot(4,2,1+(rep-1))
        plot(t,accy,'.-','LineWidth',2)
        grid on
        grid minor
        xlabel('Time (s)')
        ylabel('(m/s^2)')
        title('Accelerometer data')
        legend('y-axis')

        % Noise shift, high pass filtering, and double integration

        %% Reorient the sensor along the vertical direction

        % find an interval where the sensor is actually still

        acc_m = vecnorm(acc(:,4:6)');
        tmp = abs(acc_m-mean(acc_m));

        if (idx == 4 && rep == 1)
            mov_std_a = movstd(tmp(1:750),[25 0]);
        else
            mov_std_a = movstd(tmp(1:1500),[25 0]);
        end

        toCutStanding = mov_std_a < 0.01;
```

```
longestSequenceCutStatic = find(bwareafilt(toCutStanding == 1, 1) == true); %find the longest consecutive sequence

if ~(length(longestSequenceCutStatic) < 120)
   longestSequenceCutStatic = longestSequenceCutStatic(50:end-49);
end
hold on
plot(t(longestSequenceCutStatic),ones(size(longestSequenceCutStatic)),'.')
%       xlim([0 25])


accAvgStatic = mean(acc(longestSequenceCutStatic,4:6));
accMeas = accAvgStatic./norm(accAvgStatic);
accId = [1 0 0];

angPv = acosd(dot(accMeas,accId));
kPv = cross(accMeas,accId)./norm(cross(accMeas,accId));
qtiltPelvis = [cosd(angPv/2) sind(angPv/2)*kPv];
RtiltPelvis = quat2dcm(qtiltPelvis)';

acc_vert = zeros(N,3);

for ii = 1:N
   acc_vert(ii,:) = RtiltPelvis*acc(ii,4:6)'*9.81;
end

%% Filter the signals
acc_shift = acc_vert(:,2) - mean(acc_vert(:,2));

dt = mean(diff(t));
fs = 1/dt; % Sampling Rate
fc = 0.1/(fs/2);  % Cut off Frequency
order = 6; % 6th Order Filter
[b, a] = butter(order,fc,'high'); %Filter acc Signals

%       figure,freqz(b,a,1000,fs) % filter mask

accf_shift = filtfilt(b,a,acc_shift);
v = cumtrapz(t,accf_shift-mean(accf_shift)); %First Integration (Acceleration - Veloicty)

v_f = filtfilt(b,a,v);


d = cumtrapz(t, v_f); %Second Integration (Velocity - Displacement)


hp = subplot(3,2,3+(rep-1));
plot(t,d);
hold on
grid on
grid minor
xlabel('Time (s)')
ylabel('(m)')
title('Displacement data')

%% Average sway data

% we want to divide our signal in 12 portions (one portion for each
% increment in velocity)

n = round(N/12);
```

```
        d_mag = abs(d);


        sway_avg = arrayfun(@(i) mean(d_mag(i:i+n-1)),1:n:length(d_mag)-n+1)'; % the averaged vector

        subplot(3,2,5+(rep-1))
        plot(sway_avg,'-^')
        grid on
        grid minor
        xlabel('Portion')
        ylabel('(m)')
        title('Average displacement data')

        %% Maxima-minima

        %       [~,MaxIdx] = findpeaks(d-mean(d),'MinPeakHeight',0,'MinPeakDistance',10);
        %       [~,MinIdx] = findpeaks(-(d-mean(d)),'MinPeakHeight',0,'MinPeakDistance',10);

        for jj = 1:12
           if jj*n > N
              n = N - n*(jj-1);
           end

           app = d(n*(jj-1)+1:jj*n);

           [~,MaxIdx] = findpeaks(app-mean(app),'MinPeakDistance',10);
           [~,MinIdx] = findpeaks(-(app-mean(app)),'MinPeakDistance',10);

           MaxIdx = MaxIdx + (jj-1)*n;
           MinIdx = MinIdx + (jj-1)*n;

           Maxima = d(MaxIdx);
           Minima = d(MinIdx);

           plot(hp, t(MaxIdx), Maxima,'ro')
           plot(hp, t(MinIdx), Minima,'ko')

           maxmin = [Maxima; Minima];


           rmsmaxmin(jj,rep,idx) = mean(Maxima) - mean(Minima);


        end

        legend(hp,'y-axis','Maxima','Minima')


    end
    sgtitle(['Subj #' num2str(idx)])
end

%% Has the sway decreased or increased?

maxmin_abs = abs(rmsmaxmin);

diff_end_start = squeeze(maxmin_abs(end,:,:) - maxmin_abs(1,:,:))*100; % in cm

% positive value = increase
% negative value = decrease


%% ----------additional
```

```
% [P,f] = pwelch(acc_shift-mean(acc_shift),hamming(n/2),round(n/10),n,fs);
% figure
% plot(f,P)
```